

VILLA: Versatile Information Retrieval From Scientific Literature Using Large Language Models

Blessy Antony
Virginia Tech
Blacksburg, Virginia, USA
blessyantony@vt.edu

Amartya Dutta
Sneha Aggarwal
Virginia Tech
Blacksburg, Virginia, USA
{amartya,sengg}@vt.edu

Vasu Gatne
Virginia Tech
Blacksburg, Virginia, USA
gatne@vt.edu

Ozan Gökdemir
University of Chicago
Chicago, Illinois, USA
ogokdemir@uchicago.edu

Samantha Grimes
University of Michigan
Ann Arbor, Michigan, USA
samang@umich.edu

Adam Lauring
University of Michigan
Ann Arbor, Michigan, USA
alauring@med.umich.edu

Brian R. Wasik
Cornell University
Ithaca, New York, USA
brw72@cornell.edu

Anuj Karpatne*
Virginia Tech
Blacksburg, Virginia, USA
karpatne@vt.edu

T. M. Murali*
Virginia Tech
Blacksburg, Virginia, USA
murali@cs.vt.edu

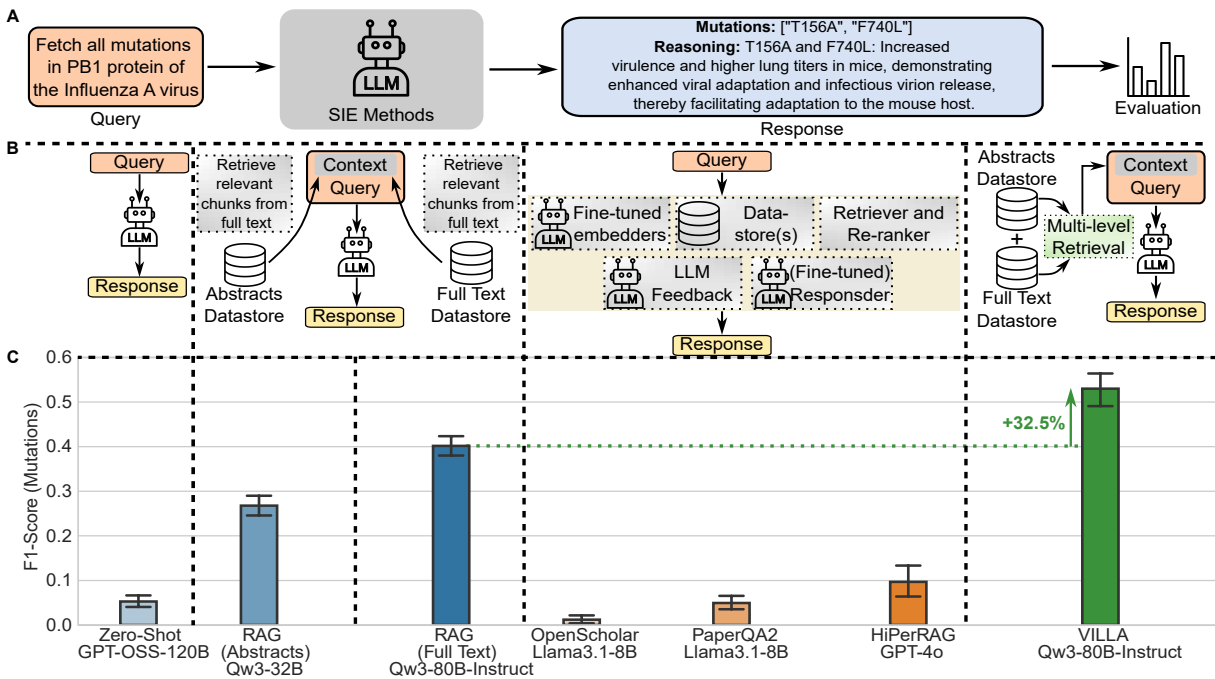


Figure 1: (A) We study an open-ended task in scientific information extraction (SIE) in the context of virology. (B) We develop VILLA, a novel two-stage method for retrieval-augmented generation (RAG). (C) VILLA outperforms zero-shot prompting, RAG- and agent-based baselines, and other state-of-the-art methods for SIE in our novel task of viral mutation extraction.

Abstract

The lack of high-quality ground truth datasets to train machine learning (ML) models impedes the potential of artificial intelligence for science (AI for science) research. Scientific information extraction (SIE) from the literature using LLMs is emerging as a powerful

approach to automate the creation of these datasets. However, existing LLM-based approaches and benchmarking studies for SIE focus on broad topics such as biomedicine and chemistry, are limited to choice-based tasks, and focus on extracting information from short and well-formatted text. The potential of SIE methods in complex, open-ended tasks is considerably under-explored. In this study, we used a domain that has been virtually ignored in

*Corresponding authors.

SIE, namely virology, to address these research gaps. We design a unique, open-ended SIE task of extracting mutations in a given virus that modify its interaction with the host. We develop a new, multi-step retrieval augmented generation (RAG) framework called VILLA for SIE. In parallel, we curate a novel dataset of 629 mutations in ten influenza A virus proteins obtained from 239 scientific publications to serve as ground truth for the mutation extraction task. Finally, we demonstrate VILLA’s superior performance using a novel and comprehensive evaluation and comparison with vanilla RAG and other state-of-the-art RAG- and agent-based tools for SIE.

Keywords

scientific information extraction, multi-step retrieval augmented generation, large language models, viral mutations

1 Introduction

Artificial Intelligence (AI) for science is accelerating research through discovery of patterns and candidate hypotheses from large-scale datasets. However, a major barrier in AI for Science is the lack of high-quality ground truth datasets to train machine learning (ML) models [5, 43]. In many fields, the relevant information is spread across the literature as unstructured text [20, 26]. It is infeasible to manually review relevant publications [6, 13, 24, 41], especially with the exponential growth in scientific literature [16, 17]. Hence, there is an urgent need for automated mechanisms to extract the findings hidden in the scientific corpus to advance AI for science.

Scientific information extraction (SIE) is the process of identifying and retrieving the desired data from the unstructured text in research publications. Advances in SIE focus on mining important data from text to enable auto-generation of tabular databases of the extracted information [13]. In recent years, the promising potential of LLMs in understanding general language and reasoning tasks have led to the development of LLM-powered tools for SIE [58]. Various approaches adopt domain specific LLMs [22, 31, 40, 49] and general purpose LLMs for SIE [3, 10, 19, 52] using zero-shot and few-shot prompting, retrieval-augmented generation (RAG), and supervised fine-tuning (SFT) (please see Appendix A for brief descriptions). Multiple studies [10, 29, 51, 52] demonstrate and compare the ability of open and closed LLM-driven tools to mine information from abstracts and full text of scientific publications. Despite the success of these methods, there are two issues.

(1) *Standard information extraction tasks are inadequate in capturing the complexity of SIE.* Existing studies evaluate the capabilities of LLMs in SIE through tasks such as named entity recognition (NER) [10, 29, 51], relation extraction (RE) [10, 29], question answering (QA), and document classification (DC). All these tasks except NER are formulated in a manner that includes the desired information in the prompt. QA explicitly provides two or more (one correct and remaining incorrect) options. IR, RE, and DC implicitly include a list of possible labels in the prompt for the LLMs to choose from. Moreover, all these tasks involve extracting information from short, clean, and well-formatted scientific text, such as a sentence or an abstract. These tasks do not realize the complexity of parsing the full text of publications and extracting the correct information.

(2) *The potential of SIE methods in complex, open-ended tasks is unknown.* Prior benchmarking pipelines evaluate the ability of several general purpose LLMs in SIE using zero-shot [10] and few-shot prompting [10, 29]. Additionally, many studies report and compare the performance of LLMs fine-tuned for SIE [10, 29]. Though the fine-tuning approach yields the best performance, the compute resources requirement for SFT of LLMs is high [10, 29]. Several RAG-based tools such as HiPerRAG [20] and agentic frameworks such as OpenScholar [2], and PaperQA2 [54] that exploit the advantages of RAG and SFT [2] have demonstrated superior performance in SIE. However, the evaluation of these methods was limited to choice-based tasks. There are no studies that evaluate and compare the performance of RAG-based methods in open-ended tasks.

In this study, we have addressed both these major research gaps. We used a highly under-explored domain in SIE, namely virology, to evaluate and demonstrate the potential of our contributions. Akin to other domains, the literature in virology has rapidly expanded (particularly since the COVID-19 pandemic) from 40,000 papers annually in 2019 to over 80,000 in subsequent years. It is imperative to extract pertinent information from this vast corpus using SIE methods and convert them into suitable formats for computational analysis to accelerate research in virology. However, there are few ground-truth datasets for SIE tasks in virology due to the paucity of annotated datasets in this domain. The standard datasets used to benchmark SIE methods span a wide range of topics such as drugs [12, 25, 27, 45], diseases [9, 15, 23], molecular biology [7, 11, 55], and general biomedical concepts [30, 44]. See Appendix B for details on the datasets. Barring LitCovid [9], the proportion of questions pertaining virology in these datasets is low (0.34% to 5.32%). LitCovid is a virology dataset focusing only on SARS-CoV-2.

In this study, (i) we designed an open-ended SIE task, i.e., the prompt we created did not ask LLMs to select from a set of pre-defined labels or answers. This task prompted the LLM to extract mutations in a given viral protein. The query did not include any concise or formatted text containing the potential answer. (ii) We proposed a novel framework called ‘VILLA’ for SIE. This two-stage RAG-based framework includes a new technique to construct the context by using abstracts to identify relevant papers and then performing an exhaustive search using the full-text of the selected publications. (iii) Our team of domain experts (virologists) manually curated a novel dataset in virology to address the lack of annotated ground truth in this domain. This dataset contained 629 mutations across ten influenza A virus proteins from 239 scientific publications to benchmark SIE methods. (iv) We demonstrated the superior performance of VILLA using a comprehensive evaluation and comparison with vanilla RAG and three other state-of-the-art (SOTA) RAG- and agent-based tools involving both open and closed LLMs to extract information from scientific publications. We leveraged our expert-curated dataset as the ground truth for these evaluations. Though we have focused on virology in this study, our proposed two-stage method VILLA can be readily adapted to other domains. Our benchmarking strategy for RAG-based tools is also generalizable, contingent on the availability of a set of papers containing the desired information and a ground-truth dataset to evaluate the findings.

2 Methodology

2.1 Problem statement

We defined an open-ended task called ‘viral mutation extraction’ to evaluate the ability of LLMs to extract information from scientific publications (Figure 1A). The goal of the task was to retrieve mutations in a given viral protein that impact virus-host interaction from one or more abstracts or full-text publications. The input included the name of a virus and one of its protein. The expected output of the task was a list of mutations in the given viral protein along with the effect of each mutation in the virus-host interaction.

With guidance from virologists, we developed a prompt template to query LLMs. In the prompt, we described the viral mutations extraction task, and provided the name of a virus and a protein of interest. The prompt also contained instructions for the LLM to respond with a JSON output containing two fields namely ‘mutations’ and ‘reasoning’ capturing the list of mutations and the effects of these mutations on virus-host interaction respectively.

We used this prompt template to query several LLMs using zero-shot prompting and SOTA SIE tools such as HiPerRAG, OpenScholar, and PaperQA2 (Appendix Figure 11). We adapted the same template for three RAG-based methods designed in this study namely RAG with abstracts, RAG with full text, and VILLA (Appendix Figure 14). Specifically, we added instructions for the LLMs to retrieve the correct mutations from only within the contextual information provided in the prompt.

2.2 Background

Our proposed framework for SIE is based on an AI technique called retrieval augmented generation (RAG). The RAG method enhances the knowledge captured in the parameters of LLMs at inference time using information from external sources. It is an optimal method of improving the performance of general purpose LLMs for domain specific tasks without incurring the overhead of compute resources required in supervised fine-tuning.

In this method, we supplement the query in the prompt with a ‘context’ that contains the correct answer. This context is constructed using relevant information from a datastore of documents of any type. The prompt also instructs the LLMs to look for the answer only in the provided context.

A RAG framework [36] typically consists of four components namely, (i) datastore (\mathcal{D}), (ii) embedder (\mathcal{E}), (iii) retriever (\mathcal{R}), and (iv) response generator (\mathcal{G}). The working of RAG with respect to the SIE experiments designed in this study is as follows:

- (1) In SIE, scientific articles act as documents to be store in the datastore.
- (2) We divided the text from publications into n chunks (c_1, c_2, \dots, c_n) of size s each.
- (3) ‘Embedder’ \mathcal{E} (we used an LLM in this study) encoded each chunk c_i into embedding vectors \mathbf{c}_i . We stored these n embeddings in a vector ‘datastore’ \mathcal{D} which served as the knowledge store for the RAG framework.
- (4) At inference time, \mathcal{E} encoded the prompt to the LLM into a vector \mathbf{p} .
- (5) The ‘retriever’ \mathcal{R} computed distances between \mathbf{p} and all chunk vectors \mathbf{c}_i in \mathcal{D} using cosine similarity as defined

in equation 1. \mathcal{R} selected the top k chunk embeddings that were closest in distance to \mathbf{p} AND whose distance was below a set threshold t . The retriever then returned the text corresponding to each of the k selected chunks. This selected text formed the context C containing external knowledge from scientific publications.

$$d(\mathbf{p}, \mathbf{c}_i) = 1 - \frac{\mathbf{p} \cdot \mathbf{c}_i}{\|\mathbf{p}\| \|\mathbf{c}_i\|} \quad (1)$$

- (6) We concatenated the selected chunks in order of increasing distances to form the context C . We inserted this context into the original prompt.
- (7) We passed the augmented query to the response generator LLM \mathcal{G} which generated a response for the prompt. We expected \mathcal{G} to extract the desired information from the context only.

2.3 Baselines

We compared the performance of our proposed framework with three baselines: zero-shot prompting and two types of RAG implementations. We summarize each method below with details in Appendix C.

2.3.1 Zero-shot prompting. We evaluated eleven general purpose LLMs using zero-shot prompting for viral mutation extraction (Section 2.1). Here, we did not augment the prompt with any additional information. Therefore, the LLMs responded using the parametric knowledge learned during their training.

2.3.2 RAG with abstracts. The datastore ($\mathcal{D}_{\mathcal{A}}$) in this method contained embeddings of the abstracts of all the 239 scientific publications in the influenza A dataset (Section 2.5).

2.3.3 RAG with full text. The datastore ($\mathcal{D}_{\mathcal{F}}$) in this method contained embeddings of 10, 327 chunks of the textual information from 239 scientific publications in the influenza A dataset (Section 2.5).

We measured the performance of seven different LLMs as embedders encoding the abstracts or full text of publications (Appendix Table 3). Similarly, we evaluated eleven distinct LLMs as responders that extracted mutation information from the context provided in the prompts.

2.4 Proposed framework: VILLA

We developed VILLA to combine the power of RAG with abstracts and RAG with full text in two steps (Algorithm 1 and Figure 2): (i) identify the relevant publications, and (ii) retrieve the accurate information from the selected publications. The different components of the method included datastore for abstracts $\mathcal{D}_{\mathcal{A}}$, datastore for chunks of textual information in publications $\mathcal{D}_{\mathcal{F}}$, embedder \mathcal{E} , retriever \mathcal{R} , and a response generator \mathcal{G} (responder). It also required a corpus of scientific publications with abstracts and full text, and a prompt p that described the information to be retrieved from the corpus. The variable parameters in the method were k_a : number of abstracts to be retrieved, k_c : number of chunks to be retrieved from each publication, and a distance threshold t .

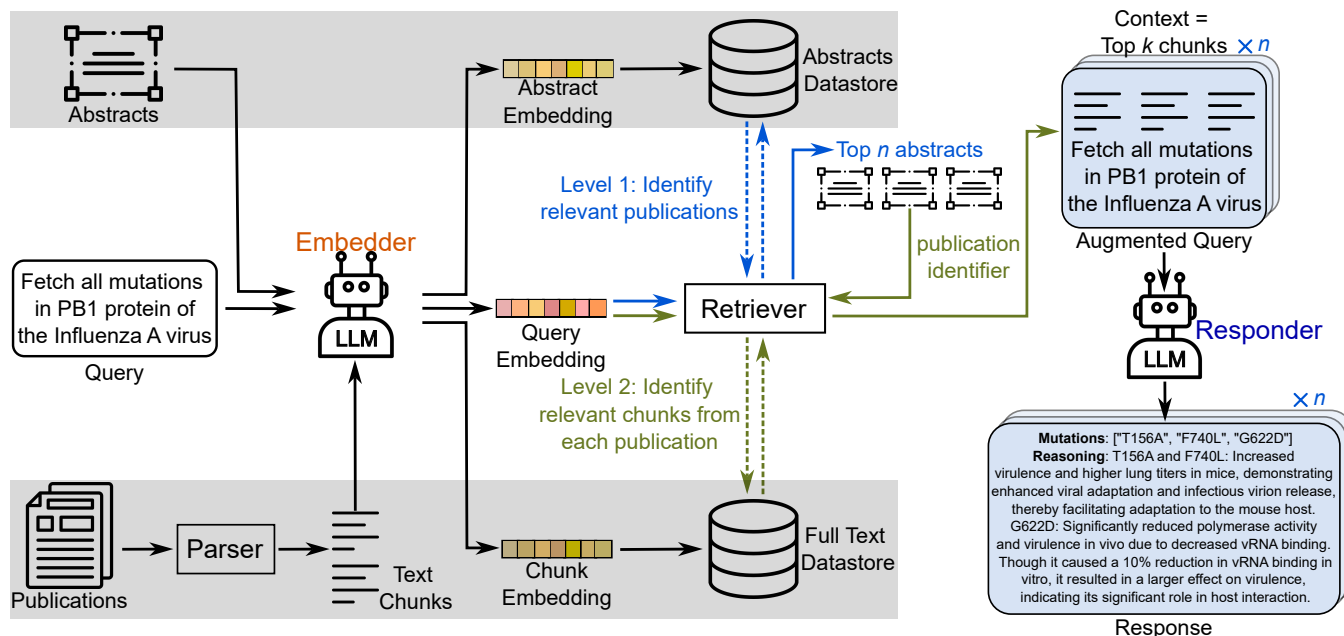


Figure 2: Overview of the multi-level RAG framework called ‘VILLA’ for SIE from publications. For a given prompt, the framework first identifies relevant publications using embeddings in the abstract datastore. Then for each selected publication, (i) retrieves relevant chunks of full text from the full text datastore, (ii) augments the input prompt with the concatenation of all the selected chunks, and (iii) generates a response for the augmented prompt.

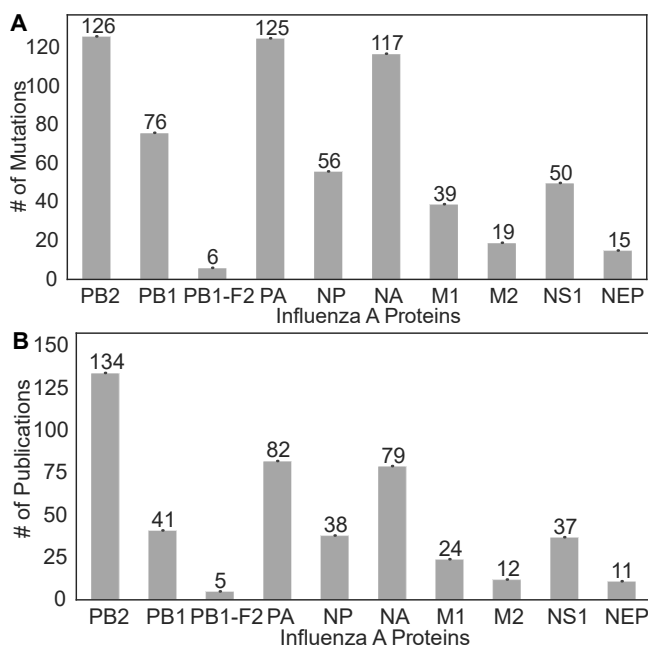


Figure 3: The number of (B) publications and (A) mutations with findings about mutations impacting virus-host interaction, in ten influenza A proteins.

2.5 Expert curated influenza A dataset

To evaluate the ability of different LLM-driven SIE methods to extract foundational knowledge in virology, we focused on influenza A virus. Influenza A viruses are extremely successful avian-borne viruses that frequently spill-over and emerge into mammalian hosts to cause outbreaks and epidemics. Influenza has been the source of novel human pandemics in 1918 (H1N1), 1957 (H2N2), 1968 (H3N2), and 2009 (swine-origin H1N1), while also contributing to millions of cases of severe illness globally each year during seasonal circulation [35]. For both pandemic human influenza and emergent lineages of virus in non-human mammals (i.e. H5N1), a multitude of studies have identified specific mutations in influenza viral proteins that demonstrate (or infer) increased risk of mammalian adaptation, virulence, and transmission to facilitate pandemic potential.

We manually curated a dataset of mutations in the influenza A virus genome from primary literature sources. The dataset focused on observed and experimental mutations with identified risk potential for mammalian adaptation. We coded all mutations for the specific amino acid change (alpha-numeric-alpha) and the viral protein as described in the text. We excluded mutations in the hemagglutinin (HA) protein as amino acid numbering schematics in the literature were inconsistent and often transformed from alignments and subtype designations [8]. There were a total of ten viral proteins categorized by major open reading frames (PB2, PB1, PA, NP, NA, M1, NS1) and known leaky ribosomal scanning or splice variants (PB1-F2, M2, NEP).

This dataset contained 629 mutations in ten influenza A virus proteins obtained from 239 unique scientific publications (Figure 3).

Algorithm 1 VILLA

Inputs: corpus of scientific publications, $\mathcal{D}_{\mathcal{A}}$, $\mathcal{D}_{\mathcal{F}}$, \mathcal{E} , \mathcal{R} , \mathcal{G} , p , k_a , k_c , and t .

Initialize: Initialize the datastores $\mathcal{D}_{\mathcal{A}}$ and $\mathcal{D}_{\mathcal{F}}$.

- 1: **for** each publication in the corpus **do**
- 2: Embed the abstract using \mathcal{E} and store the abstract embedding with the corresponding publication identifier in $\mathcal{D}_{\mathcal{A}}$.
- 3: Break the full text of the publication into chunks of equal size with overlap.
- 4: Embed each chunk using \mathcal{E} and store the chunk embedding with the corresponding publication identifier in $\mathcal{D}_{\mathcal{F}}$.
- 5: **end for**
- 6: **function** VILLA($\mathcal{D}_{\mathcal{A}}$, $\mathcal{D}_{\mathcal{F}}$, \mathcal{E} , \mathcal{R} , \mathcal{G} , k_a , k_c , p)
- 7: Embed the prompt p using \mathcal{E} .
- 8: Level 1 retrieval: Retrieve the k_a abstracts from $\mathcal{D}_{\mathcal{A}}$ with the closest cosine distance (within threshold t) to the prompt embedding.
- 9: **for** each of the selected abstracts **do**
- 10: Level 2 retrieval: Retrieve k_c chunks of publication, corresponding to the selected abstract, from $\mathcal{D}_{\mathcal{F}}$ with the closest cosine distance (within threshold t) to the prompt embedding. These chunks form the context.
- 11: Concatenate the retrieved context with the original prompt p to augment it.
- 12: Query the responder \mathcal{G} with the augmented prompt.
- 13: Store the mutations and reasoning from the response of \mathcal{G} .
- 14: **end for**
- 15: **return** Lists of mutations and reasonings from LLMs for all selected publications.
- 16: **end function**

2.6 Evaluation strategy

In this study, we used the influenza A dataset as ground truth (Section 2.5) to evaluate the different SIE methods. Each prompt to the LLMs included one of the ten different viral proteins in the ground truth dataset. We formulated two different types of evaluations:

2.6.1 Evaluation of retrieved context. We evaluated the embedder LLMs in the RAG with abstracts and full text, and the proposed VILLA methods (Appendix C.5, Appendix Table 3). The ground truth dataset (Section 2.5) included lists of relevant publications for each viral protein. We used these lists to gauge the correctness of the context. For each prompt that contained a viral protein, we captured the publication corresponding to each of the top k abstracts (RAG with abstracts and VILLA) or chunks (RAG with full text) that composed the context. We compared this list of retrieved publications with those corresponding to the input protein in the ground truth dataset. We computed the precision, recall, and F1-score of the retrieved context for each protein (prompt).

The retriever selected the top k chunks closest to the embedding of the prompt. Thus, this evaluation of the context helped to compare the different embedder LLMs.

2.6.2 Evaluation of extracted information. Our ground truth dataset consisted of a list of mutations impacting virus-host interaction for

every viral protein. In the SIE task, we prompted the responder models (Appendix C.4, Appendix Table 2) to respond with a list of mutations in given viral protein. Further we defined the symbolic representation of mutations as $\langle \text{original amino acid} \rangle \langle \text{position} \rangle \langle \text{changed amino acid} \rangle$ where $\langle \text{position} \rangle$ denoted the position where the mutation occurs in the viral protein sequence, $\langle \text{original amino acid} \rangle$ is the alphabet representing the amino acid at that position in the viral protein sequence, and $\langle \text{changed amino acid} \rangle$ is the alphabet representing the changed amino acid. For example, “A123C” is a mutation of amino acid “A” to “C” at position “123”. We compared the list of mutations in the response of the LLMs with the mutations corresponding to the input protein in the ground truth dataset (Section 2.5). We computed the precision, recall, and F1-score of the retrieved mutations for each protein (prompt).

2.6.3 Qualitative evaluation. Two virologists who earned their doctoral degrees in virology evaluated the ‘reasoning’ component in the LLM responses. We designed a five-point rubric (Appendix D) in five categories for the qualitative evaluation of LLM responses, with one being the lowest score and five the highest. Rubric categories were clarity, conciseness, correctness, citations/context, and contribution. We developed a web-based user interface where the domain experts could view and evaluate the responses in an unbiased manner (Appendix D.2). We defined each category as a question for the evaluator in order to further standardize the qualitative considerations.

3 Experimental Setup

We evaluated a wide range of LLMs as response generators using zero-shot prompting and RAG. In addition to the generators, we also evaluated different embedding LLMs as embedders in RAG. Finally we benchmarked three state-of-the-art RAG- and agent-based tools for SIE.

3.1 Response generators for zero-shot prompting and RAG-based methods

We evaluated eleven general purpose LLMs using the SIE task (Section 2.1) and the influenza A dataset (Section 2.5). We used two closed models namely OpenAI’s o1 and GPT-4o, and nine open models including GPT-OSS 120B, ZAI-GLM4.5, two models from the DeepSeek family, two from Llama, and three from Qwen3 (Appendix C.4, Appendix Table 2).

3.2 Embedders for RAG-based methods

The three RAG-based frameworks (Sections 2.3.2, 2.3.3, 2.4) contained an additional LLM-based component called embedder (Section 2.2). We compared the performance of seven different textual embedders that encoded text input into vectors.

3.2.1 General purpose embedders. We used one closed namely Open AI’s text-embedding-3-large, and four open embedders including Llama 3.1:8B, Qwen3-Embedding:8B, Google’s Embedding Gemma:300M, and Embedding Mistral-Q4KM from SalesForce (Appendix C.5). The proportion of scientific content is low in the training dataset of a typical LLM. General-purpose encoding LLMs underperform in tasks involving scientific text [20].

3.2.2 Embedders for scientific publications. We also evaluated two additional embedder LLMs pretrained explicitly on textual information from scientific publications. PubMedBERT is a Bidirectional Encoder Representations from Transformers (BERT) model pretrained on 14 million abstracts from PubMed [22]. MedCPT consists of query encoder and document encoder which are two independent PubMedBERT models. These two encoders were further pretrained using contrastive learning on 255 million query-article pairs from PubMed search logs. During this contrastive learning, the model learned to maximize the similarity between a query and its related article(s). [31].

3.3 Other frameworks

We evaluated three state-of-the-art methods for SIE:

- (i) OpenScholar [2]: enhanced RAG framework with a large-scale scientific datastore consisting of 45 million open-access papers;
- (ii) PaperQA2 [54]: a scientific question-answering framework that utilises an agentic framework; and
- (iii) HiPerRAG [20]: a modular, open-source high-performance computing (HPC) framework for scaling RAG across the full scientific pipeline.

Please see Appendix C for details.

We compared the performances of all frameworks with Llama 3.1:8B as the response generator (responder) in a RAG-based setup. We also assessed additional flavors of PaperQA2, HiPerRAG, and VILLA with different LLMs as responders and varying compositions of the datastores in the respective frameworks. OpenScholar [2] is powered through a fine-tuned Llama 3.1:8B model and a datastore of 45 million open-access scientific papers. In PaperQA2, we leveraged the capabilities of the full agentic framework with Llama3.1:70B as the agent and Llama3.1:8B as the query model (referred to as ‘Agents’ mode in Table 1). We also evaluated an ablation of PaperQA2 comprising only the RAG capabilities (‘RAG’ mode). PaperQA2 enables users to build a custom datastore to perform SIE and we used the 239 influenza A publications in order to mimic the setup in VILLA. For HiPerRAG [20], we implemented a high-performance RAG framework using ~ 440K full-text microbiology publications to construct the datastore. We also created an additional datastore of the 239 influenza A articles and evaluated HiPerRAG with this smaller set of papers.

4 Results

We prompted LLMs to respond with the mutations in a given viral protein. An experiment in this study included ten such prompts, one for each influenza A protein (Section 2.5). We repeated each experiment five times to ensure reliability of the LLM responses. For each method, we report the distribution of metrics across these fifty experiments (Section 2.6).

4.1 Performance of zero-shot prompting

We evaluated eleven LLMs in SIE using zero-shot prompting for viral mutation extraction in influenza A virus (Appendix E.1). For each model, we averaged the precision, recall, and F1-scores over all proteins. The Open AI open source model GPT-oss-120B had the highest average F1-score of 0.10 ± 0.11 across all proteins and

iterations, followed by Open AI o1 (\$) with 0.10 ± 0.12 (Figure 4). However, the average recall was low, ranging from 0.003 (Deepseek-R1-Distill-Qwen-32B) to 0.07 (Z.ai-GLM4.5-Air). On average, the models were able to accurately retrieve only 4.26% of the mutations across all proteins. We concluded that zero-shot prompting was not an effective approach for retrieving influenza A viral mutations. General purpose LLMs are not exposed to domain specific knowledge in scientific publications during pretraining [20]. The lack of information about virology in the parametric knowledge of the LLMs motivated us to explore RAG-based methods for SIE.

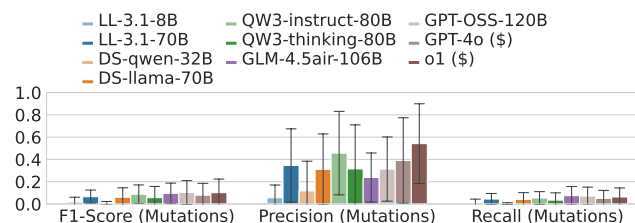


Figure 4: Distribution of the F1-scores, precision, and recall of eleven LLMs in identifying mutations across ten proteins in influenza A virus using zero-shot prompting. Each bar height and error bar corresponds to the mean and standard deviation of the distribution of scores across ten proteins and five iterations, respectively. Abbreviations: LL, Llama; DS, DeepSeek; QW3, Qwen.

4.2 Viral mutation extraction using RAG with abstracts

Next, we set up a RAG framework using abstracts (Section 2.3.2) of all 239 scientific publications in the influenza A dataset (Section 2.5).

4.2.1 Evaluation of the extracted mutations. We evaluated the retrieved mutations at two levels: (i) with respect to the mutations for each protein in the ground truth dataset, and (ii) with respect to context, that is, with respect to only those ground truth mutations present in the publications of the abstracts selected as part of the context. Note that for each protein, the latter set of mutations was a subset of the former.

Qwen3-32B had the overall best performance with average precision, recall, and F1-scores of 0.82 ± 0.13 , 0.16 ± 0.06 , and 0.27 ± 0.08 respectively (Figure 5, Appendix Figure 15). Irrespective of the precision, we observed low recall and F1-scores across all models suggesting the abstracts in these publications did not contain the mutations we were seeking.

For all responder LLMs, the precision with respect to context and overall precision scores were strictly identical with the exception of one protein (NA) where the overall precision was larger in some iterations. The recall with respect to context was larger than the overall recall scores. This result suggested that the responder did not hallucinate correct mutations that were not present within the context. The distribution of all scores for each of the ten influenza A proteins are in Appendix Figures 17 and 18.

4.2.2 Evaluation of the selected abstracts. We evaluated the ability of this framework to retrieve the correct abstracts. For a given

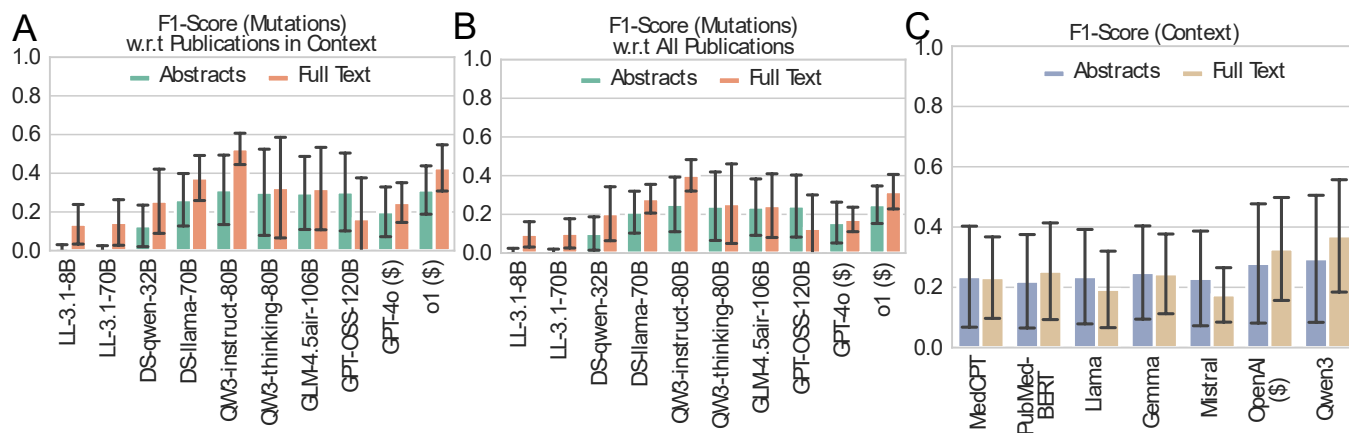


Figure 5: Distribution of the F1-scores with respect to the (A) ground truth mutations in the publications represented in the context in the prompt and (B) the ground truth mutations in all the publications. (C) Distribution of the F1-scores of the retriever in the two RAG frameworks in identifying abstracts relevant to each of the ten proteins in influenza A virus. The retriever is evaluated using seven different embedding LLMs. Each bar height and error bar corresponds to the mean and standard deviation of the distribution of scores across ten proteins and five iterations, respectively. Abbreviations: LL, Llama; DS, DeepSeek; QW3, Qwen.

protein in the prompt, we compared the publications represented in the context with those corresponding to the protein in the ground truth dataset. The average F1-scores across all ten influenza A proteins are shown in Figure 5C while precision and recall scores are in Appendix Figure 15. The distribution of all three metrics on a per protein basis is shown in Appendix Figure 16. The mean recall of the publications in the context across all proteins ranged from 0.54 (MedCPT) to 0.70 (Qwen3-Embedding:8B). However, the range of mean precision was low: from 0.16 (PubMedBERT) to 0.22 (Qwen3-Embedding:8B). Qwen3-Embedding:8B had the best performance with mean F1-score of 0.29 ± 0.21 , followed by Open AI’s text-embedding-3-large (\$) model with 0.28 ± 0.20 . We chose the Qwen3-Embedding:8B model with the highest F1-score for further analysis.

Next, we sought to understand the reason for the low precision. We computed the cosine distances between the Qwen3-Embedding:8B model’s embedding of a prompt for viral mutation extraction for a influenza A protein, and the embeddings of the abstracts from publications corresponding to the protein (relevant). Similarly, we measured the distance between the prompt and abstracts of all remaining publications (non-relevant to the given protein) in the ground truth dataset. We compared the distributions of distances of relevant and non-relevant abstracts for all ten influenza A proteins (Appendix Figure 24). The mean distance of the relevant abstracts was significantly less than that of the non-relevant abstracts for eight out of the ten proteins (Mann-Whitney U test). However, the p -values may be underestimated because of the difference in the number of relevant and non-relevant abstracts for each protein. We observed a lower p -value for proteins with fewer relevant abstracts. Despite the high overlap between the two distributions we selected the open-weight Qwen3-Embedding:8B LLM as the embedder in the RAG framework for further analysis because it had the highest mean F1-score.

4.3 Viral mutation extraction using RAG with full text

We configured another RAG framework using the full textual information in the publications (Section 2.3.3). We divided the text in each publication into overlapping chunks. Unlike RAG with abstracts, the datastore in this method contained embeddings of 10,327 chunks of full text from 239 influenza A publications.

4.3.1 Evaluation of the extracted mutations. As described in Section 4.2.1, we computed the precision, recall, and F1-scores of the retrieved mutations with respect to the ground truth mutations in the context (Appendix Figure 21) and overall ground truth (Appendix Figure 20). Qwen3-Next-80B-A3B-Instruct model had the highest mean F1-score of 0.41 ± 0.08 (Figure 5). The precision values with respect to ground truth in context were almost equal to the overall precision; and the recall values with respect to context were higher than the corresponding overall values (Appendix Figure 15). This pattern, similar to the observation in RAG with abstracts, demonstrated the absence of LLM hallucinations of correct mutations.

4.3.2 Evaluation of the context. We evaluated list of publications represented in the context through individual chunks. Similar to RAG with abstracts, Qwen3-Embedding:8B had the best performance with average F1-score of 0.37 ± 0.19 , followed by Open AI’s text-embedding-3-large (\$) model with 0.33 ± 0.17 (Figure 5C). We chose the open source Qwen3-Embedding:8B LLM as the embedder for further analysis again.

4.4 Viral mutation extraction using VILLA

In this novel two-step RAG (Section 2.4), we harnessed the benefits of higher recall of relevant publications in the context using RAG with abstracts, and higher recall of viral mutations using RAG with full text. Since the first level of selecting publications

using abstracts was identical to the retrieval process in RAG with abstracts (Section 4.2.2), we directly evaluate and discuss the performance of VILLA in viral mutation extraction. Similar to the previous two RAG frameworks, we used the Qwen3-Embedding:8B LLM as the embedder for subsequent evaluation of LLMs as responders in multi-level RAG.

4.4.1 Evaluation of the extracted mutations. We measured the precision, recall, and F1-scores of retrieved mutations with respect to the ground truth mutations corresponding to the provided context. We also computed the metrics with respect to all the ground truth mutations from all publications in datastore for a given protein (Figure 6). Appendix figures 22 and 23 contain the distribution of these metrics at the individual protein level. VILLA improved on the shortcoming of lower recall in the RAG with abstracts and full text methods. Qwen3-Next-80B-A3B-Instruct had the highest mean F1-score of 0.53 ± 0.13 with similar mean precision (0.58 ± 0.17) and recall (0.50 ± 0.14) values.

4.4.2 Selecting optimal number of abstracts and chunks in VILLA. We performed hyperparameter tuning to determine the optimal number of abstracts (k_a) and chunks from each publication (k_c) to be selected in the two retrieval steps of the multi-level RAG algorithm (Algorithm 1, Section 2.4). In this analysis, we used the LLMs with highest mean F1-score in selecting publications and retrieving mutations, as embedder and responder respectively. Thus, we used ‘Qwen3-Embedding-8B’ (Section 4.2.2) to compute embeddings and ‘Qwen3-Next-80B-A3B-Instruct’ to generate the response (Section 4.4.1). We used the influenza A dataset for viral mutation extraction in ten proteins with several combination of values for k_a and k_c (Appendix Figure 26). First, we explored six different values for k_a from the set of {5, 10, 20, 40, 80, 160} with k_c fixed at 160. Next, we set $k_a = 160$ and varied $k_c = \{5, 10, 20, 40, 80, 160\}$.

In VILLA, k_a controlled the number of publications selected in the first retrieval step (Section 2.4). A larger value of k_a enabled the framework to improve the recall but impacted the precision of the extracted mutations. Starting at $k = 5$ (precision= 0.44 ± 0.40), we observed highest mean precision of across all proteins at $k_a = 20$ (0.64 ± 0.20) which decreased by $\sim 11\%$ at $k_a = 160$ (0.57 ± 0.13). The recall steadily increased from 0.09 ± 0.10 to 0.50 ± 0.14 as we varied k_a from 5 to 160. Therefore there was an increasing trend in F1-scores as well from 0.14 ± 0.15 to 0.52 ± 0.11 with increasing k_a .

However, the values of k_c did not influence the performance of multi-level RAG method. The mean F1-scores of retrieved mutations ranged from 0.52 ± 0.12 to 0.52 ± 0.11 when we varied k_c from 5 to 160.

4.5 Benchmarking RAG-based frameworks for viral mutation extraction

We compared the F1-scores of nine different LLMs as response generators (responders) for SIE using zero-shot prompting, two RAG-based methods, and VILLA. Our multi-level RAG-based method significantly outperformed zero-shot prompting and RAG with abstracts for eight out of nine LLMs (Appendix Figure 27). Similarly, VILLA was significantly better than RAG with full text for six LLMs. Finally, we benchmarked state-of-the-art RAG-based tools for SIE

namely, OpenScholar [2], PaperQA2 [54], and HiPerRAG [20] (Figure 1C, Table 1, Appendix Figure 28).

4.6 Qualitative evaluation

To assess the model outputs for their reasoning and insight, we devised a qualitative assessment to be performed by subject-matter experts (e.g., virologists). Our rubric utilized five metrics along two general dimensions: language/syntax (Correctness, Conciseness, Clarity) and biological significance (Citations and Contribution). See Appendix D for details. We coalesced the respondent scores across each metric into a single profile for each model (Figure 7). We observed that VILLA diverged from the other models on the language/syntax dimension. Most models performed comparably while VILLA lagged in Conciseness score. In contrast, VILLA was comparable to other models along the dimension of biological relevance, with substantially improved performance of Citations.

Although we have established the substantial improvement of VILLA in the quantitative measure of recall (Table 1), our subject-matter experts observed limited improvement of VILLA in ‘Contribution’ (biological relevance) or ‘Correctness’ (general language). We discuss the limitations of VILLA highlighted by these trends in Section 6.

5 Contribution to Virology

Viruses are the most diverse and abundant biological entities with about 10^{31} viral particles in nature [34, 48]. As many as 60% of novel human infectious diseases since 1940 have been caused by viruses originating in animals [18, 33, 57]. Challenges in virology include foundational understanding of virus biology and pathogenesis, the development of therapeutic vaccines and anti-viral drugs, in addition to the development of predictive models of virus emergence and outbreak dynamics. Computational methods, including ML models, have aided in the acceleration of research in virology [4, 28, 39, 50]. There is a critical need for automated tools to accurately extract desired information from the vast scientific corpus and create structured datasets in virology that can drive research in AI for virology.

To develop LLM-based SIE methods for virology, we used the influenza A virus to establish a controlled experiment of text retrieval on mutations in its proteins. We selected this virus since it has a rich literature over six decades. In contrast, the research literature for a multitude of zoonotic- and pandemic-risk viruses are more dispersed and siloed. Unlike quantitative datasets in tabular and figure-borne formats, viral genome mutations (and their described impact on virus function) represent text-based information retrieval that is more nuanced. Therefore, any automated system of retrieval would be of significant value. Further, this data is critical to foundational questions of viral pathogenesis and emergence risk and may facilitate the development of new predictive models. Our results demonstrate that complex and multi-step methods are necessary to build a proper SIE protocol, thus tempering any over-confident rush to zero-shot methods. We also provide a framework for improved design and the need for iterative LLM pretraining data in domain-specific scientific literature.

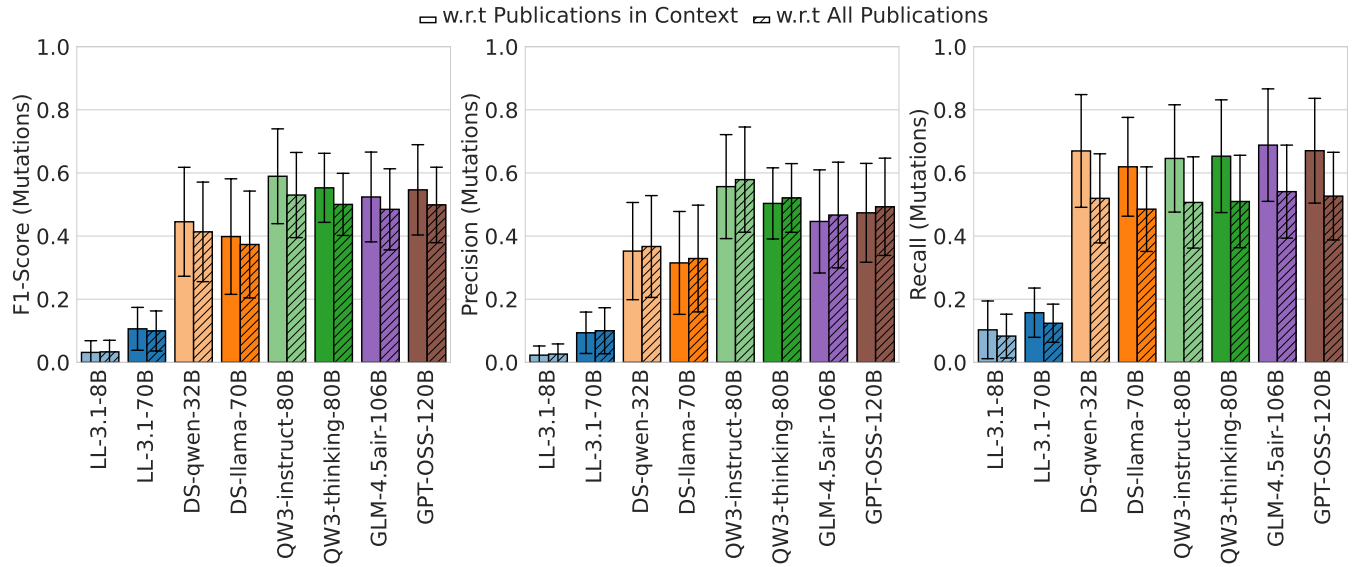


Figure 6: Distribution of the precision, recall, and F1-scores with respect to the ground truth in the publications represented in the context in the prompt and the ground truth (hatched bars). The scores are for eight LLMs evaluated in identifying mutations across ten proteins in influenza A virus using VILLA.

SIE Method	Response Generator	Datatore (# papers)	F1-Score	Precision	Recall
OpenScholar	Llama 3.1:8B	Semantic scholar (45 million)	0.02 ± 0.08	0.04 ± 0.07	0.01 ± 0.02
PaperQA2 (RAG mode)	Llama 3.1:8B	Influenza A (239)	0.07 ± 0.08	0.27 ± 0.30	0.05 ± 0.06
PaperQA2 (Agent mode)	Llama 3.1:8B	Influenza A (239)	0.05 ± 0.06	0.43 ± 0.44	0.03 ± 0.04
HiPerRAG	Llama 3.1:8B	ASM journal (~ 440K)	0.01 ± 0.02	0.04 ± 0.07	0.01 ± 0.02
HiPerRAG	GPT-4o	ASM journal (~ 440K)	0.09 ± 0.12	0.50 ± 0.42	0.05 ± 0.07
HiPerRAG	GPT-4o	Influenza A (239)	0.10 ± 0.12	0.52 ± 0.39	0.06 ± 0.07
VILLA (ours)	Llama 3.1:8B	Influenza A (239)	0.03 ± 0.04	0.03 ± 0.03	0.08 ± 0.07
VILLA (ours)	Qwen3-Instruct:80B	Influenza A (239)	0.53±0.13	0.57±0.17	0.51±0.14

Table 1: Mean and standard deviation of the distribution of the F1-scores, precision, and recall scores of OpenScholar, PaperQA2, HiPerRAG, and VILLA frameworks in retrieving mutations of influenza A viral proteins. Each distribution is across five iterations of viral mutation extraction for each of the ten influenza A proteins.

6 Limitations and Ethical Considerations

Since our research is on SIE, we do not see any implications related to consent or potential misuse. The data we use is present in the primary literature. We accessed the full text of relevant publications through institutional subscriptions to the relevant journals. We note that there may be an inherent bias in which proteins are studied by scientists [21]. In the case of influenza A virus, many more functionally-relevant mutations have been identified in the NA, PA, PB1, PB2 proteins. (Figure 3).

Our quantitative results, F1-score of 0.53 ± 0.13 , precision of 0.57 ± 0.17 , and recall of 0.51 ± 0.14 (Table 1), indicate that there is substantial ground for increasing the number of mutations retrieved correctly from the ground truth literature. Our analysis of the abstracts retrieved in the first step of multi-level RAG demonstrated substantial overlap between the distribution of distances from the query to abstracts relevant to the corresponding protein

and distribution of distances from the query to other abstracts (Appendix Figure 24). There is scope for considerable improvement in separating these distance distributions.

Our qualitative results (Figure 7) highlight additional limitations. The relatively poor evaluation of VILLA in ‘Conciseness’ results from its concatenation of the outputs from iterative queries for each relevant publication. We also observed limited improvement of VILLA in ‘Contribution’ (biological relevance) or ‘Correctness’ (general language). This trend is likely a function of a limitation in our design where rubric-based qualitative evaluation of results can diverge from a quantitative score such as recall. Subject-matter experts do not inherently know the number of potential mutations of a protein present in the ground truth dataset. Therefore, an output of a small number of mutations (if accurate and accompanied by properly given context) cannot outscore a model result that correctly recalls even 3- or 4-fold greater mutations from the ground truth. While we can observe this disparity given our known ground truth

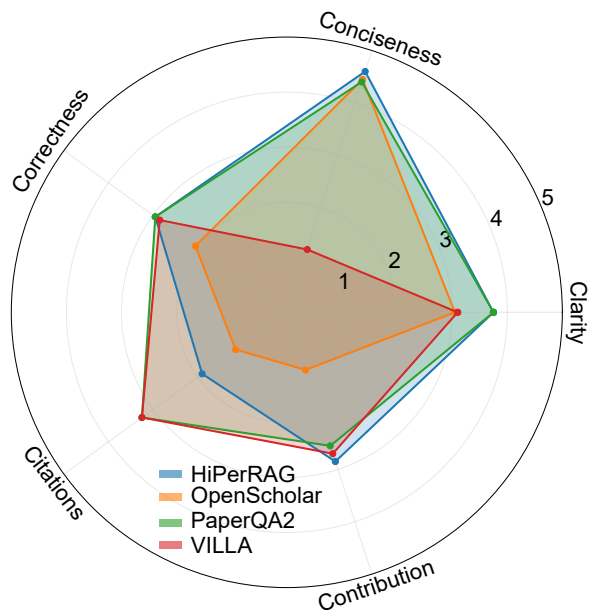


Figure 7: Qualitative evaluation of the reasoning in model responses for the viral mutation extraction task. Metric scores (5-point rubric) for each viral protein ($n=10$) were coalesced into a single profile for each model framework.

dataset, SIE methods applied to topics without such a dataset may be challenged to demonstrate high recall in any limited qualitative assessment that may be desired. We hypothesize that this deficit, and a general tax from lack of conciseness, may have caused the parity of VILLA with other models along the ‘biological relevance’ dimension.

7 Conclusion

In this study, we defined a novel SIE task for viral mutation extraction. We designed a novel multi-level RAG method for SIE called VILLA. Further, we curated a dataset of 629 mutations across ten influenza A virus proteins from 239 scientific publications. We used this ground-truth dataset to evaluate a wide range of LLMs using baseline SIE methods such as zero-shot prompting and RAG- and agent-based tools. We also demonstrated that VILLA outperformed these baselines and had higher recall and F1-scores when compared to SOTA methods such as OpenScholar, PaperQA2, and HiperRAG.

We envision two future expansions of this study. First, a major challenge is to improve the performance (precision, recall, F1-score) of RAG-based approaches for our SIE task. One possibility may be to use a different prompt to select the right context. We may also consider NER methods to retrieve the correct chunks of textual information from publications. Second, SIE methods typically involve querying the LLMs with one prompt at a time for a given task instance. In our case, the number of queries to the response generator LLM in the proposed multi-level RAG approach was directly proportional to the number of abstracts selected in the first retrieval step. An important research question to address is systematically

reducing the number of queries to LLMs in open-ended SIE tasks without compromising the quality of results.

Acknowledgments

National Science Foundation awards CCF-2412389 and CCF-2200045, the Pandemic Prediction and Prevention Destination Area at Virginia Tech, and the College of Engineering at Virginia Tech supported this research work.

References

- [1] OpenAI (2024). 2024. GPT-4o System Card. <https://openai.com/index/gpt-4o-system-card/>.
- [2] Akari Asai, Jacqueline He, Rulin Shao, Weijia Shi, Amanpreet Singh, Joseph Chee Chang, Kyle Lo, Luca Soldaini, Sergey Feldman, Mike D’arcy, David Wadden, Matt Latzke, Mingyang Tian, Pan Ji, Shengyan Liu, Hao Tong, Bohao Wu, Yanyu Xiong, Luke Zettlemoyer, Graham Neubig, Dan Weld, Doug Downey, Wen-tau Yih, Pang Wei Koh, and Hannaneh Hajishirzi. 2024. OpenScholar: Synthesizing Scientific Literature with Retrieval-augmented LMs. arXiv:2411.14199 doi:10.48550/arXiv.2411.14199
- [3] Samy Ateia, Udo Kruschwitz, Melanie Scholz, Agnes Koschmider, and Moayad Almoahishi. 2026. LLM-Based Information Extraction to Support Scientific Literature Research and Publication Workflows. In *New Trends in Theory and Practice of Digital Libraries*, Wolf-Tilo Balke, Koralka Golub, Yannis Manolopoulos, Kostas Stefanidis, Zheyang Zhang, Trond Aalberg, and Paolo Manghi (Eds.). Springer Nature Switzerland, Cham, 90–99. doi:10.1007/978-3-032-06136-2_9
- [4] Karim Beguir, Marcin J. Skwark, Yunguan Fu, Thomas Pierrot, Nicolas Lopez Carranza, Alexandre Laterre, Ibtissem Kadri, Abir Korched, Anna U. Lowgard, Bonny Gaby Lui, Bianca Sanger, Yunpeng Liu, Asaf Poran, Alexander Muik, and Uğur Şahin. 2023. Early Computational Detection of Potential High-Risk SARS-CoV-2 Variants. *Computers in Biology and Medicine* 155 (March 2023), 106618. doi:10.1016/j.combiomed.2023.106618
- [5] Philipp Berens, Kyle Cranmer, Neil D. Lawrence, Ulrike von Luxburg, and Jessica Montgomery. 2023. AI for Science: An Emerging Agenda. arXiv:2303.04217 doi:10.48550/arXiv.2303.04217
- [6] Arthur Brack, Jennifer D’Souza, Anett Hoppe, Søren Auer, and Ralph Ewerth. 2020. Domain-Independent Extraction of Scientific Concepts from Research Articles. In *Advances in Information Retrieval*, Joemon M. Jose, Emine Yilmaz, João Magalhães, Pablo Castells, Nicola Ferro, Mário J. Silva, and Flávio Martins (Eds.). Springer International Publishing, Cham, 251–266. doi:10.1007/978-3-030-45439-5_17
- [7] Àlex Bravo, Janet Piñero, Nuria Queralt-Rosinach, Michael Rautschka, and Laura I. Furlong. 2015. Extraction of Relations between Genes and Diseases from Text and Large-Scale Data Analysis: Implications for Translational Research. *BMC Bioinformatics* 16, 1 (Feb. 2015), 55. doi:10.1186/s12859-015-0472-9
- [8] David F. Burke and Derek J. Smith. 2014. A Recommended Numbering Scheme for Influenza A HA Subtypes. *PLoS One* 9, 11 (2014), e112302. doi:10.1371/journal.pone.0112302
- [9] Qingyu Chen, Alexis Allot, and Zhiyong Lu. 2021. LitCovid: An Open Database of COVID-19 Literature. *Nucleic Acids Research* 49, D1 (Jan. 2021), D1534–D1540. doi:10.1093/nar/gkaa952
- [10] Qingyu Chen, Yan Hu, Xueqing Peng, Qianqian Xie, Qiao Jin, Aidan Gilson, Maxwell B. Singer, Xuguang Ai, Po-Ting Lai, Zhizheng Wang, Vipina K. Keloth, Kalpana Raja, Jimin Huang, Huan He, Fongci Lin, Jingcheng Du, Rui Zhang, W. Jim Zheng, Ron A. Adelman, Zhiyong Lu, and Hua Xu. 2025. Benchmarking Large Language Models for Biomedical Natural Language Processing Applications and Recommendations. *Nature Communications* 16, 1 (April 2025), 3280. doi:10.1038/s41467-025-56989-2
- [11] Nigel Collier, Tomoko Ohta, Yoshimasa Tsuruoka, Yuka Tateisi, and Jin-Dong Kim. 2004. Introduction to the Bio-entity Recognition Task at JNLPBA. In *Proceedings of the International Joint Workshop on Natural Language Processing in Biomedicine and Its Applications (NLPBA/BioNLP)*, Nigel Collier, Patrick Ruch, and Adeline Nazarenko (Eds.). COLING, Geneva, Switzerland, 73–78.
- [12] Gamal Crichton, Sampo Pyysalo, Billy Chiu, and Anna Korhonen. 2017. A Neural Network Multi-Task Learning Approach to Biomedical Named Entity Recognition. *BMC Bioinformatics* 18, 1 (Aug. 2017), 368. doi:10.1186/s12859-017-1776-8
- [13] John Dagdelen, Alexander Dunn, Sanghoon Lee, Nicholas Walker, Andrew S. Rosen, Gerbrand Ceder, Kristin A. Persson, and Anubhav Jain. 2024. Structured Information Extraction from Scientific Text with Large Language Models. *Nature Communications* 15, 1 (Feb. 2024), 1418. doi:10.1038/s41467-024-45563-x
- [14] DeepSeek-AI. 2025. DeepSeek-R1: Incentivizing Reasoning Capability in LLMs via Reinforcement Learning. arXiv:2501.12948 [cs.CL] <https://arxiv.org/abs/2501.12948>

- [15] Rezarta Islamaj Doğan, Robert Leaman, and Zhiyong Lu. 2014. NCBI Disease Corpus: A Resource for Disease Name Recognition and Concept Normalization. *Journal of Biomedical Informatics* 47 (Feb. 2014), 1–10. doi:10.1016/j.jbi.2013.12.006
- [16] Said El Shamieh and Alain Chebly. 2024. Trends in Scientific Publishing: Does Quantity Compromise Quality in Life Sciences and Medicine? *Systematic Reviews* 13, 1 (Oct. 2024), 249. doi:10.1186/s13643-024-02668-0
- [17] Michael Fire and Carlos Guestrin. 2019. Over-Optimization of Academic Publishing Metrics: Observing Goodhart’s Law in Action. *GigaScience* 8, 6 (May 2019), giz053. doi:10.1093/gigascience/giz053
- [18] Diego Forni, Rachele Cagliani, Mario Clerici, and Manuela Sironi. 2022. Disease-Causing Human Viruses: Novelty and Legacy. *Trends in Microbiology* 30, 12 (Dec. 2022), 1232–1242. doi:10.1016/j.tim.2022.07.002
- [19] Gabriel Lino Garcia, João Renato Ribeiro Manesco, Pedro Henrique Paiola, Lucas Miranda, Maria Paola de Salvo, and João Paulo Papa. 2024. A Review on Scientific Knowledge Extraction using Large Language Models in Biomedical Sciences. arXiv:2412.03531 [cs.CL]. doi:10.26434/chemrxiv-2024-03531
- [20] Ozan Gokdemir, Carlo Siebenschuh, Alexander Brace, Azton Wells, Brian Hsu, Kyle Hippe, Priyanka Setty, Aswathy Ajith, J. Gregory Pauloski, Varuni Sastry, Sam Foreman, Huihuo Zheng, Heng Ma, Bharat Kale, Nicholas Chia, Thomas Gibbs, Michael Papka, Thomas Brettin, Francis Alexander, Anima Anandkumar, Ian Foster, Rick Stevens, Venkatram Vishwanath, and Arvind Ramanathan. 2025. HiPerRAG: High-Performance Retrieval Augmented Generation for Scientific Insights. In *Proceedings of the Platform for Advanced Scientific Computing Conference (PASC ’25)*. Association for Computing Machinery, New York, NY, USA, 1–13. doi:10.1145/3732775.3733586
- [21] Steven Grudman, Carlos Madrid-Aliste, and Andras Fiser. 2025. Overcoming Research Bias: The Untapped Potential of Biomedically Important but Understudied Proteins. *iScience* 28, 9 (Sept. 2025), 113210. doi:10.1016/j.isci.2025.113210
- [22] Yu Gu, Robert Tinn, Hao Cheng, Michael Lucas, Naoto Usuyama, Xiaodong Liu, Tristan Naumann, Jianfeng Gao, and Hoifung Poon. 2021. Domain-Specific Language Model Pretraining for Biomedical Natural Language Processing. *ACM Trans. Comput. Healthcare* 3, 1 (Oct. 2021), 2:1–2:23. doi:10.1145/3458754
- [23] Douglas Hanahan and Robert A. Weinberg. 2011. Hallmarks of Cancer: The Next Generation. *Cell* 144, 5 (March 2011), 646–674. doi:10.1016/j.cell.2011.02.013
- [24] Mark A. Hanson, Pablo Gómez Barreiro, Paolo Crossetto, and Dan Brockington. 2024. The Strain on Scientific Publishing. *Quantitative Science Studies* 5, 4 (Nov. 2024), 823–843. doi:10.1162/qss_a_00327
- [25] Maria Herrero-Zazo, Isabel Segura-Bedmar, Paloma Martínez, and Thierry Declercq. 2013. The DDI Corpus: An Annotated Corpus with Pharmacological Substances and Drug–Drug Interactions. *Journal of Biomedical Informatics* 46, 5 (Oct. 2013), 914–920. doi:10.1016/j.jbi.2013.07.011
- [26] Edward C. Holmes, Florian Krammer, and Felicia D. Goodrum. 2024. Virology—The next Fifty Years. *Cell* 187, 19 (Sept. 2024), 5128–5145. doi:10.1016/j.cell.2024.07.025
- [27] Rezarta Islamaj Doğan, Sun Kim, Andrew Chatr-aryamontri, Chih-Hsuan Wei, Donald C Comeau, Rui Antunes, Sérgio Matos, Qingyu Chen, Aparna Elangovan, Nagesh C Panyam, Karin Verspoor, Hongfang Liu, Yanshan Wang, Zhuang Liu, Berna Altinel, Zehra Melce Hüsünbeyi, Arzucan Özgür, Aris Fergadis, Chen-Kai Wang, Hong-Jie Dai, Tung Tran, Ramakanth Kavuluru, Ling Luo, Albert Steppi, Jinfeng Zhang, Jinchuan Qu, and Zhiyong Lu. 2019. Overview of the BioCreative VI Precision Medicine Track: Mining Protein Interactions and Mutations for Precision Medicine. *Database* 2019 (Jan. 2019), bay147. doi:10.1093/database/bay147
- [28] Jumpei Ito, Adam Strange, Wei Liu, Gustav Joas, Spyros Lytras, and Kei Sato. 2025. A Protein Language Model for Exploring Viral Fitness Landscapes. *Nature Communications* 16, 1 (May 2025), 4236. doi:10.1038/s41467-025-59422-w
- [29] Bernal Jimenez Gutierrez, Nikolas McNeal, Clayton Washington, You Chen, Lang Li, Huan Sun, and Yu Su. 2022. Thinking about GPT-3 In-Context Learning for Biomedical IE? Think Again. In *Findings of the Association for Computational Linguistics: EMNLP 2022*, Yoav Goldberg, Zornitsa Kozareva, and Yue Zhang (Eds.). Association for Computational Linguistics, Abu Dhabi, United Arab Emirates, 4497–4512. doi:10.18653/v1/2022.findings-emnlp.329
- [30] Qiao Jin, Bhuwan Dhingra, Zhengping Liu, William Cohen, and Xinghua Lu. 2019. PubMedQA: A Dataset for Biomedical Research Question Answering. In *Proceedings of the 2019 Conference on Empirical Methods in Natural Language Processing and the 9th International Joint Conference on Natural Language Processing (EMNLP-IJCNLP)*, Kentaro Inui, Jing Jiang, Vincent Ng, and Xiaojun Wan (Eds.). Association for Computational Linguistics, Hong Kong, China, 2567–2577. doi:10.18653/v1/D19-1259
- [31] Qiao Jin, Won Kim, Qingyu Chen, Donald C Comeau, Lana Yeganova, W John Wilbur, and Zhiyong Lu. 2023. MedCPT: Contrastive Pre-trained Transformers with large-scale PubMed search logs for zero-shot biomedical information retrieval. *Bioinformatics* 39, 11 (2023), btad651.
- [32] Jeff Johnson, Matthijs Douze, and Hervé Jégou. 2019. Billion-scale similarity search with GPUs. *IEEE Transactions on Big Data* 7, 3 (2019), 535–547.
- [33] Kate E. Jones, Nikkita G. Patel, Marc A. Levy, Adam Storeygard, Deborah Balk, John L. Gittleman, and Peter Daszak. 2008. Global Trends in Emerging Infectious Diseases. *Nature* 451, 7181 (Feb. 2008), 990–993. doi:10.1038/nature06536
- [34] Eugene V. Koonin, Mart Krupovic, and Valerian V. Dolja. 2023. The Global Virome: How Much Diversity and How Many Independent Origins? *Environmental Microbiology* 25, 1 (2023), 40–44. doi:10.1111/1462-2920.16207
- [35] Florian Krammer, Gavin J. D. Smith, Ron A. M. Fouchier, Malik Peiris, Katherine Kedzierska, Peter C. Doherty, Peter Palese, Megan L. Shaw, John Treanor, Robert G. Webster, and Adolfo Garcia-Sastre. 2018. Influenza. *Nature Reviews Disease Primers* 4, 1 (June 2018), 3. doi:10.1038/s41572-018-0002-y
- [36] Patrick Lewis, Ethan Perez, Aleksandra Piktus, Fabio Petroni, Vladimir Karpukhin, Naman Goyal, Heinrich Küttler, Mike Lewis, Wen-tau Yih, Tim Rocktäschel, Sebastian Riedel, and Douwe Kiela. 2020. Retrieval-Augmented Generation for Knowledge-Intensive NLP Tasks. In *Advances in Neural Information Processing Systems*, Vol. 33. Curran Associates, Inc., Red Hook, NY, USA, 9459–9474.
- [37] Jiao Li, Yueping Sun, Robin J. Johnson, Daniela Sciaky, Chih-Hsuan Wei, Robert Leaman, Allan Peter Davis, Carolyn J. Mattingly, Thomas C. Wieggers, and Zhiyong Lu. 2016. BioCreative V CDR Task Corpus: A Resource for Chemical Disease Relation Extraction. *Database* 2016 (Jan. 2016), baw068. doi:10.1093/database/baw068
- [38] Zhao Li, Qiang Wei, Liang-Chin Huang, Jianfu Li, Yan Hu, Yao-Shun Chuang, Jianping He, Avisha Das, Vipina Kuttichi Keloth, Yuntao Yang, Chiamaka S Diala, Kirk E Roberts, Cui Tao, Xiaoqian Jiang, W Jim Zheng, and Hua Xu. 2024. Ensemble Pretrained Language Models to Extract Biomedical Knowledge from Literature. *Journal of the American Medical Informatics Association* 31, 9 (Sept. 2024), 1904–1911. doi:10.1093/jamia/ocae061
- [39] Benjamin J Livesey and Joseph A Marsh. 2020. Using Deep Mutational Scanning to Benchmark Variant Effect Predictors and Identify Disease Mutations. *Molecular Systems Biology* 16, 7 (July 2020), e9380. doi:10.15252/msb.20199380
- [40] Renqian Luo, Liai Sun, Yingce Xia, Tao Qin, Sheng Zhang, Hoifung Poon, and Tie-Yan Liu. 2022. BioGPT: Generative Pre-Trained Transformer for Biomedical Text Generation and Mining. *Briefings in Bioinformatics* 23, 6 (Nov. 2022), bbac409. doi:10.1093/bib/bbac409
- [41] Lili Ma, Wei Pan, and Jiali Si. 2024. Bibliometric Analysis of Virology Advancements in the 21st Century. *Virologica Sinica* 39, 6 (Dec. 2024), 977–980. doi:10.1016/j.virs.2024.08.009
- [42] Rui Meng, Ye Liu, Shafiq Rayhan Joty, Caiming Xiong, Yingbo Zhou, and Semih Yavuz. 2024. SFR-Embedding-Mistral-Enhance Text Retrieval with Transfer Learning. *Salesforce AI Research Blog*. <https://www.salesforce.com/blog/sfr-embedding/>
- [43] Research Intelligence Nature. 2025. AI for Science 2025. *Nature, Research Intelligence* 4 (2025).
- [44] Anastasios Nentidis, Konstantinos Bougiatiotis, Anastasia Krithara, Georgios Paliouras, and Ioannis Kakadiaris. 2017. Results of the Fifth Edition of the BioASQ Challenge. In *Proceedings of the 16th BioNLP Workshop*, Kevin Bretonnel Cohen, Dina Demner-Fushman, Sophia Ananiadou, and Junichi Tsujii (Eds.). Association for Computational Linguistics, Vancouver, Canada, 48–57. doi:10.18653/v1/W17-2306
- [45] Benjamin Nye, Junyi Jessy Li, Roma Patel, Yinfei Yang, Iain Marshall, Ani Nenkova, and Byron Wallace. 2018. A Corpus with Multi-Level Annotations of Patients, Interventions and Outcomes to Support Language Processing for Medical Literature. In *Proceedings of the 56th Annual Meeting of the Association for Computational Linguistics (Volume 1: Long Papers)*, Iryna Gurevych and Yusuke Miyao (Eds.). Association for Computational Linguistics, Melbourne, Australia, 197–207. doi:10.18653/v1/P18-1019
- [46] OpenAI, Sandhini Agarwal, Lama Ahmad, Jason Ai, Sam Altman, Andy Applebaum, Edwin Arbus, Rahul K. Arora, Yu Bai, Bowen Baker, Haiming Bao, Boaz Barak, Ally Bennett, Tyler Bertao, Nivedita Brett, Eugene Brevdo, Greg Brockman, Sebastien Bubeck, Che Chang, Kai Chen, Mark Chen, Enoch Cheung, Aidan Clark, Dan Cook, Marat Dukhan, Casey Dvorkak, Kevin Fives, Vlad Fomenko, Timur Garipov, Kristian Georgiev, Mia Glaese, Tarun Gogineni, Adam Goucher, Lukas Gross, Katia Gil Guzman, John Hallman, Jackie Hehir, Johannes Heidecke, Alec Helyar, Haitang Hu, Romain Huet, Jacob Huh, Saachi Jain, Zach Johnson, Chris Koch, Irina Kofman, Dominik Kundel, Jason Kwon, Volodymyr Kyrlyov, Elaine Ya Le, Guillaume Leclerc, James Park Lennon, Scott Lessans, Mario Lezcano-Casado, Yuanzhi Li, Zhuohan Li, Ji Lin, Jordan Liss, Lily, Liu, Jiancheng Liu, Kevin Lu, Chris Lu, Zoran Martinovic, Lindsay McCallum, Josh McGrath, Scott McKinney, Aidan McLaughlin, Song Mei, Steve Mostovoy, Tong Mu, Gideon Myles, Alexander Neitz, Alex Nichol, Jakub Pachocki, Alex Paino, Dana Palmie, Ashley Pantuliano, Giambattista Parascandolo, Jongsoo Park, Leher Pathak, Carolina Paz, Ludovic Peran, Dmitry Pimenov, Michelle Pokrass, Elizabeth Proehl, Huida Qiu, Gaby Raila, Filippo Raso, Hongyu Ren, Kimmy Richardson, David Robinson, Bob Rotsted, Hadi Salman, Suvansh Sanjeev, Max Schwarzer, D. Sculley, Harshit Sikchi, Kendal Simon, Karan Singhal, Yang Song, Dane Stuckey, Zhiqing Sun, Philippe Tillet, Sam Toizer, Foivos Tsimpouraki, Nikhil Vyas, Eric Wallace, Xin Wang, Miles Wang, Olivia Watkins, Kevin Weil, Amy Wendling, Kevin Whinnery, Cedric Whitney, Hannah Wong, Lin Yang, Yu Yang, Michihiro Yasunaga, Kristen Ying, Wojciech Zaremba, Wenting Zhan, Cyril Zhang, Brian Zhang, Eddie Zhang, and Shengjia Zhao. 2025. Gpt-Oss-120b & Gpt-Oss-20b Model Card.

- arXiv:2508.10925 doi:10.48550/arXiv.2508.10925
- [47] OpenAI, Aaron Jaech, Adam Kalai, Adam Lerer, Adam Richardson, Ahmed El-Kishky, Aiden Low, Alec Helyar, Aleksander Madry, Alex Beutel, Alex Carney, Alex Ifimie, Alex Karpenko, Alex Tachard Passos, Alexander Neitz, Alexander Prokofiev, Alexander Wei, Allison Tam, Ally Bennett, Ananya Kumar, Andre Saraiva, Andrea Vallone, Andrew Duberstein, Andrew Kondrich, Andrew Mishchenko, Andy Applebaum, Angela Jiang, Ashvin Nair, Barret Zoph, Behrooz Ghorbani, Ben Rossen, Benjamin Sokolowsky, Boaz Barak, Bob McGrew, Borys Minaiev, Botao Hao, Bowen Baker, Brandon Houghton, Brandon McKinzie, Brydon Eastman, Camillo Lugaresi, Cary Bassin, Cary Hudson, Chak Ming Li, Charles de Bourcy, Chelsea Voss, Chen Shen, Chong Zhang, Chris Koch, Chris Orsinger, Christopher Hesse, Claudia Fischer, Clive Chan, Dan Roberts, Daniel Kappler, Daniel Levy, Daniel Selsam, David Dohan, David Farhi, David Mely, David Robinson, Dimitris Tsipras, Doug Li, Dragos Oprica, Eben Freeman, Freddie Sulit, Geoff Salmon, Giambattista Parascandolo, Gildas Chabot, Grace Zhao, Greg Brockman, Guillaume Leclerc, Hadi Salman, Haiming Bao, Hao Sheng, Hart Andrin, Hessam Bagherinezhad, Hongyu Ren, Hunter Lightman, Hyung Won Chung, Ian Kivlichan, Ian O'Connell, Ian Osband, Ignasi Clavera Gilaberte, Ilge Akkaya, Ilya Kostrikov, Ilya Sutskever, Irina Kofman, Jakub Pachocki, James Lennon, Jason Wei, Jean Harb, Jerry Twore, Jiacheng Feng, Jiahui Yu, Jiayi Weng, Jie Tang, Jieqi Yu, Joaquin Quiñero Candela, Joe Palermo, Joel Parish, Johannes Heidecke, John Hallman, John Rizzo, Jonathan Gordon, Jonathan Uesato, Jonathan Ward, Joost Huizinga, Julie Wang, Kai Chen, Kai Xiao, Karan Singhal, Karina Nguyen, Karl Cobbe, Katy Shi, Kayla Wood, Kendra Rimbach, Keren Gulemberg, Kevin Liu, Kevin Lu, Kevin Stone, Kevin Yu, Lama Ahmad, Lauren Yang, Leo Liu, Leon Maksin, Leyton Ho, Liam Fedus, Lilian Weng, Linden Li, Lindsay McCallum, Lindsey Held, Lorenz Kuhn, Lukas Kondraciuk, Lukasz Kaiser, Luke Metz, Madelaine Boyd, Maja Trebacz, Manas Joglekar, Mark Chen, Marko Tintor, Mason Meyer, Matt Jones, Matt Kaufer, Max Schwarzer, Meghan Shah, Mehmet Yatbaz, Melody Y. Guan, Mengyuan Xu, Mengyuan Yan, Mia Glaese, Mianna Chen, Michael Lampe, Michael Malek, Michele Wang, Michelle Fradin, Mike McClay, Mikhail Pavlov, Miles Wang, Mingxuan Wang, Mira Murati, Mo Bavarian, Mostafa Rohaninejad, Nat McAleese, Neil Chowdhury, Neil Chowdhury, Nick Ryder, Nikolas Tezak, Noam Brown, Ofir Nachum, Oleg Boiko, Oleg Murk, Olivia Watkins, Patrick Chao, Paul Ashbourne, Pavel Izmailov, Peter Zhokhov, Rachel Dias, Rahul Arora, Randall Lin, Rapha Gontijo Lopes, Raz Gaon, Reah Miyara, Reimar Leike, Renny Hwang, Rhythm Garg, Robin Brown, Roshan James, Rui Shu, Ryan Cheu, Ryan Greene, Saachi Jain, Sam Altman, Sam Toizer, Sam Toyer, Samuel Miserendino, Sandhini Agarwal, Santiago Hernandez, Sasha Baker, Scott McKinney, Scottie Yan, Shengjia Zhao, Shengli Hu, Shibani Santurkar, Shraman Ray Chaudhuri, Shuyuan Zhang, Siyuan Fu, Spencer Papay, Steph Lin, Suchir Balaji, Suvansh Sanjeev, Szymon Sidor, Tal Broda, Aidan Clark, Tao Wang, Taylor Gordon, Ted Sanders, Tejal Patwardhan, Thibault Sottiaux, Thomas Degry, Thomas Dimson, Tianhao Zheng, Timur Garipov, Tom Stasi, Trapit Bansal, Trevor Creech, Troy Peterson, Tyna Eloundou, Valerie Qi, Vineet Kosaraju, Vinnie Monaco, Vitchyr Pong, Vlad Fomenko, Weiyi Zheng, Wenda Zhou, Wes McCabe, Wojciech Zaremba, Yann Dubois, Yinghai Lu, Yining Chen, Young Cha, Yu Bai, Yuchen He, Yuchen Zhang, Yunyun Wang, Zheng Shao, and Zhuohan Li. 2024. OpenAI O1 System Card. arXiv:2412.16720 doi:10.48550/arXiv.2412.16720
- [48] David Paez-Espino, Emiley A. Eloee-Fadros, Georgios A. Pavlopoulos, Alex D. Thomas, Marcel Huntemann, Natalia Mikhailova, Edward Rubin, Natalia N. Ivanova, and Nikos C. Kyrpides. 2016. Uncovering Earth's Virome. *Nature* 536, 7617 (Aug. 2016), 425–430. doi:10.1038/nature19094
- [49] Long N. Phan, James T. Anibal, Hieu Tran, Shaurya Chanana, Erol Bahadroglu, Alec Peltekian, and Grégoire Altan-Bonnet. 2021. SciFive: a text-to-text transformer model for biomedical literature. arXiv:2106.03598 [cs.CL] <https://arxiv.org/abs/2106.03598>
- [50] Simone Rancati, Giovanna Nicora, Laura Bergomi, Tommaso Mario Buonocore, Daniel M Czyn, Enea Parimbelli, Riccardo Bellazzi, Marco Salemi, Mattia Prosperi, and Simone Marini. 2025. SARITA: A Large Language Model for Generating the S1 Subunit of the SARS-CoV-2 Spike Protein. *Briefings in Bioinformatics* 26, 4 (July 2025), bbaf384. doi:10.1093/bib/bbaf384
- [51] Mahsa Shamsabadi, Jennifer D'Souza, and Sören Auer. 2024. Large Language Models for Scientific Information Extraction: An Empirical Study for Virology. In *Findings of the Association for Computational Linguistics: EACL 2024*, Yvette Graham and Matthew Purver (Eds.). Association for Computational Linguistics, St. Julian's, Malta, 374–392.
- [52] Kinyi Shang, Xu Liao, Zhicheng Ji, and Wenpin Hou. 2025. Benchmarking Large Language Models for Genomic Knowledge with GeneTuring. *Briefings in Bioinformatics* 26, 5 (Sept. 2025), bbaf492. doi:10.1093/bib/bbaf492
- [53] Carlo Siebenschuh, Kyle Hippe, Ozan Gokdemir, Alexander Brace, Arham Khan, Khalid Hossain, Yadu Babuji, Nicholas Chia, Venkatram Vishwanath, Rick Stevens, Arvind Ramanathan, Ian Foster, and Robert Underwood. 2025. AdaParse: An Adaptive Parallel PDF Parsing and Resource Scaling Engine. arXiv:2505.01435 [cs.IR] <https://arxiv.org/abs/2505.01435>
- [54] Michael D. Skarlinski, Sam Cox, Jon M. Laurent, James D. Braza, Michaela Hinks, Michael J. Hammerling, Manvitha Ponnampati, Samuel G. Rodrigues, and Andrew D. White. 2024. Language Agents Achieve Superhuman Synthesis of Scientific Knowledge. arXiv:2409.13740 doi:10.48550/arXiv.2409.13740
- [55] Larry Smith, Lorraine K. Tanabe, Rie Johnson nee Ando, Cheng-Ju Kuo, I-Fang Chung, Chun-Nan Hsu, Yu-Shi Lin, Roman Klinger, Christoph M. Friedrich, Kuzman Ganchev, Manabu Torii, Hongfang Liu, Barry Haddow, Craig A. Struble, Richard J. Povinelli, Andreas Vlachos, William A. Baumgartner, Lawrence Hunter, Bob Carpenter, Richard Tzong-Han Tsai, Hong-Jie Dai, Feng Liu, Yifei Chen, Chengjie Sun, Sophia Katrenko, Pieter Adriaans, Christian Blaschke, Rafael Torres, Mariana Neves, Preslav Nakov, Anna Divoli, Manuel Maña-López, Jacinto Mata, and W. John Wilbur. 2008. Overview of BioCreative II Gene Mention Recognition. *Genome Biology* 9, 2 (Sept. 2008), S2. doi:10.1186/gb-2008-9-s2-s2
- [56] Qwen Team. 2025. Qwen3 Technical Report. arXiv:2505.09388 [cs.CL] <https://arxiv.org/abs/2505.09388>
- [57] Robin A. Weiss and Neeraja Sankaran. 2022. Emergence of Epidemic Diseases: Zoonoses and Other Origins. *F1000Prime Rep* 11, 2 (Jan. 2022). <https://connect.h1.co/prime/reports/b/11/2>
- [58] Derong Xu, Wei Chen, Wenjun Peng, Chao Zhang, Tong Xu, Xiangyu Zhao, Xian Wu, Yefeng Zheng, Yang Wang, and Enhong Chen. 2024. Large Language Models for Generative Information Extraction: A Survey. *Frontiers of Computer Science* 18, 6 (Nov. 2024), 186357. doi:10.1007/s11704-024-40555-y

A Related Work

Initial works in SIE employed rule-based techniques, regular expressions, convolutional neural networks (CNN), and natural language processing methods such as recurrent neural networks (RNN) and long-short term memory (LSTM) [13, 38]. SciFive [49], PubMedBERT [22], BioGPT [40], and MedCPT [31] are some examples of LLMs that are pretrained on scientific literature in PubMed and used for scientific information extraction (SIE). These LLMs generate higher quality embeddings for biomedical text.

Common approaches for SIE include zero-shot prompting, few-shot prompting, retrieval augmented generation (RAG), and supervised fine-tuning (SFT). In zero-shot prompting, we pose the task to the LLM in the form of a prompt in natural language. Here we do not retrain the LLM in any way or provide information in the form of labeled (or solved) examples. We rely on the ability of an LLM to steer its generated response based on guidance in the input prompt available via natural language. Few-shot prompting involves adding one or more solved examples of the task within the prompt with the intention of guiding the LLM on how to respond. In the RAG framework, an external tool is used to select pieces of text that are relevant to the query and may contain the potential answer from an external knowledge store. This retrieved ‘context’ is used to augment the original prompt. The LLMs are expected to respond with the correct answer retrieved from the context. SFT includes leveraging a ground truth dataset of question-answer pairs related to the task to fine-tune the parameters of LLM. SFT updates the model weights through backward propagation of the loss incurred while identifying the correct answers to the queries in the ground truth dataset.

B Benchmark Datasets for Scientific Information Extraction

There are several standard datasets that are commonly used to benchmark LLMs in their ability to extract information from scientific publications. These datasets are set up for different types of scientific information extraction (SIE) tasks such as named entity recognition (NER), information extraction (IR), relation extraction (RE), document classification (DC), and question answering (QA). We describe in brief the different datasets used to evaluate LLMs in each of these tasks. We also mention the proportion of ‘virus-related’ records in these datasets from the Chen et al. [10] benchmarking study that included all standard datasets. We tagged records containing any of the following terms as a virus-related record: ‘virus’, ‘viruses’, ‘viral’, ‘virulent’, ‘virulence’.

B.1 Named entity recognition

BC5-Chemical [12, 22, 37]. Based on the BioCreative V Chemical-Disease Relation corpus of 1,500 PubMed abstracts with annotations. The dataset contained 13,938 records with chemicals (drugs) as named entities in these abstracts. There were 95 (proportion= 0.68%) virus-related records in the dataset.

BC5-Disease [12, 22, 37]. Based on the BioCreative V Chemical-Disease Relation corpus to create a dataset of 1,500 PubMed abstracts with annotations. The dataset contained 13,938 records

with diseases as named entities in these abstracts. There were 95 (proportion= 0.68%) virus-related records in the dataset.

NCBI-Disease [15, 22]. Based on the Natural Center for Biotechnology Information Disease corpus containing 793 PubMed abstracts with annotations. The dataset contained 7,287 records annotated with 790 unique disease entities. There were 25 (proportion= 0.34%) virus-related records in the dataset.

BC2GM [12, 22, 55]. Based on the Biocreative II Gene Mention corpus. The dataset contained 24,583 records with manually annotated gene entities. Each record consisted of a sentence from PubMed abstracts and a set of gene entities mentioned in the sentence.

JNLBPA [11, 12, 22]. Based on the Natural Language Processing in Biomedicine and Its Applications Shared Task corpus. The dataset 59,963 records of PubMed abstracts with labels as names of entities (such as cell line, cell type, DNA, protein, and RNA) in molecular biology.

B.2 Information extraction

EBM PICO [22, 45]. Based on the Evidence-Based Medicine corpus of ~ 5,000 abstracts on clinical trials in PubMed with annotations. There are 440,852 records with abstracts and their corresponding annotations for the Participants, Intervention, Comparator, and Outcome.

B.3 Relation extraction

ChemProt [22, 27]. Based on the Chemical Protein Interaction corpus containing PubMed abstracts with annotations. The dataset had 48,223 records where each record was a sentence from an abstract and a corresponding label with one of the following six interaction types between chemical and protein entities: ‘Upregulator’, ‘Downregulator’, ‘Agonist’, ‘Antagonist’, ‘Substrate’, and ‘False’ (for all other interactions). There were 207 (proportion= 0.43%) virus-related records in the dataset.

DDI [22, 25]. Based on the Drug-Drug Interaction corpus containing PubMed abstracts with annotations. The dataset had 31,784 records where each record was a sentence from an abstract. The boolean label in the record denoted whether the given sentence contained a drug-drug interaction. There were 241 (proportion= 0.76%) virus-related records in the dataset.

GAD [7, 22]. Based on the Genetic Association Database corpus containing sentences from PubMed abstracts with their corresponding gene-disease associations. The dataset has 5,330 records where each record is a sentence from an abstract labeled with a gene-disease associations.

B.4 Document classification

HoC [22, 23]. Based on the Hallmarks of Cancer corpus containing PubMed abstracts with their binary labels denoting the discussion of different cancer hallmarks. The dataset had 1,580 records of PubMed abstracts annotated with binary labels for ten cancer hallmarks. There were 99 (proportion= 6.27%) virus-related records in the dataset.

LitCovid [9]. The dataset contained abstracts of COVID-19 related publications from PubMed. Each article was labeled with one or more of the following eight categories using manual or computational methods: ‘General Information’, ‘Mechanism’, ‘Transmission’, ‘Diagnosis’, ‘Treatment’, ‘Prevention’, ‘Case Report’, and ‘Epidemic Forecasting’. All the 33,699 records in the dataset pertained to virology.

B.5 Question answering

PubMedQA [30]. The dataset had 211,769 records, each containing text from a PubMed abstract and a research question. The label (‘Yes’, ‘No’, or ‘Maybe’) in every record was the answer to the question based on the reference text. There were 11,275 (proportion=5.32%) virus-related records in the dataset.

BioASQ [44]. The dataset was adapted from the BioASQ corpus and had 885 records. Each record contained text from a PubMed abstract and a research question. The label (‘Yes’ or ‘No’) in every record was an answer to the question based on the reference text.

Existing studies benchmark LLMs using standard datasets spanning a wide range of topics such as drugs (BioCreative V Chemical-Disease Relation [12], EBM PICO [45], ChemProt [27], DDI [25]), diseases (NCBI-Disease [15], HoC [23], LitCovid [9]), molecular biology (BC2GM [55], JNLBPA [11], GAD [7]), and general biomedical concepts (PubMedQA [30], and BioASQ [44]).

C Baseline Implementation

C.1 Zero-shot prompting

We evaluated eleven (two closed and nine open) general purpose LLMs using zero-shot prompting for viral mutation extraction.

C.2 RAG with abstracts

An embedder LLM encoded these abstracts and stored the vector representations in a datastore. We set the chunk size $s = 5,000$ tokens (each token corresponds to a character) to avoid splitting a single abstract into two or more chunks. Thus, \mathcal{D}_A contained embeddings of 239 abstract chunks. At inference time, the embedder encoded the prompt. We set $k_a = 150$ and distance threshold= 0.5 to retrieve the top 150 abstracts closest and within a radius of 0.5 to a given prompt in the embedding space. Setting $k_a = 150$ allowed the framework to capture information from a wide range of abstracts while adhering to the limitations on the size of the prompt enforced by the LLMs. Further, we set the threshold $t = 0.5$ to avoid selecting less relevant or non-relevant abstracts. A retriever computed which abstracts had embeddings that were within a cosine distance of at most 0.5 to that of the prompt’s embedding. The retriever chose a maximum of 150 abstracts. These selected abstracts constituted the context. We augmented the original prompt with the concatenation of the selected abstracts. A responder LLM received this augmented prompt containing instructions to extract the mutations for the given protein from the abstracts in the context.

C.3 RAG with full text

We first used the ‘marker’ tool¹ to parse the PDF files of the publications and extracted only the textual information from the main

¹<https://github.com/datalab-to/marker>

sections in the paper. We did not include the abstract, references, or supplementary material. We divided the full text of each publication into chunks of size 1,000 tokens with an overlap of 100 tokens. Thus, \mathcal{D}_F contained 10,327 chunks of text from 239 publications. We set $k_c = 150$ and distance threshold = 0.5 to retrieve the top 150 chunks closest and within a radius of 0.5 to a given prompt in the embedding space.

C.4 Response generator models

Appendix Table 2 lists the different LLMs evaluated as response generators in zero-shot evaluation, RAG with abstracts, RAG with full text, and VILLA SIE methods.

C.5 Embedder models

Appendix Table 3 contains the various embedding LLMs evaluated as embedders in RAG with abstracts, RAG with full text, and the proposed multi-level RAG frameworks.

C.6 Other frameworks

OpenScholar. This enhanced RAG framework consists of a large-scale scientific datastore consisting of 45 million open-access papers, dense retrievers further pre-trained to fetch relevant passages from datastore with scientific contents, cross-encoder re-ranker that was fine-tuned to select passages most relevant to the input query, and response generation using customized and off-the-shelf LLMs. It also includes improvement of responses through iterative self-feedback triggering retrieval and inference. We evaluated OpenScholar² through its user interface.

PaperQA2. This model is a scientific question-answering framework that utilizes an agentic framework where an agent LLM acts as the ‘Tool Selector’ and dynamically plans, selects tools, iteratively gathers and evaluates evidence, and decides when it has sufficient support to generate and terminate an answer. In its simple RAG mode, PaperQA2 executes a fixed, linear pipeline in which tools are invoked in a predefined order (search → evidence gathering → answer generation).

HiPerRAG. This modular, open-source high-performance computing (HPC) framework scales RAG across the full scientific pipeline, including PDF parsing, semantic chunking, embedding, retrieval, and answer generation. The modular design of the framework enabled customization of each pipeline component, including AdaParse for PDF parsing [53], PubMedBERT for semantic chunk boundary detection [22], SFR-Mistral-Embedding for chunk encoding [42], and GPT-4o and LLaMA-3.1-8B as response generators. In this study, we used HiPerRAG to construct a datastore of 448,650 scientific articles in microbiology curated in PDF format. The framework first parsed and extracted raw text using AdaParse [53], a distributed PDF parsing pipeline that produces tokenizer-ready text at scale.

To address context-window constraints and restrict inference inputs to relevant content, we applied semantic chunking to the extracted corpus. This distributed chunking process ran on 8 NVIDIA A100 GPUs for approximately 18 hours, yielding 4,500,220 cogent and self-contained semantic text chunks. We used PubMedBERT [22] to encode sentence buffers during chunk boundary detection.

²<https://opencilm.allen.ai/>

Model Developer	Model Name	Model Type	HuggingFace Model Name
DeepSeek-AI	DeepSeek-R1-Distill-Llama-70B [14]	Reasoning	deepseek-ai/DeepSeek-R1-Distill-Llama-70B
	DeepSeek-R1-Distill-Qwen-32B [14]	Reasoning	deepseek-ai/DeepSeek-R1-Distill-Qwen-32B
Meta	Llama-3.1-8B	Instruction	meta-llama/Llama-3.1-8B
	DeepSeek-R1-Distill-Qwen-32B	Reasoning	deepseek-ai/DeepSeek-R1-Distill-Qwen-32B
Qwen	Qwen3-32B	Instruction	Qwen/Qwen3-32B
	Qwen3-Next-80B-A3B-Instruct [56]	Instruction	Qwen/Qwen3-Next-80B-A3B-Instruct
	Qwen3-Next-80B-A3B-Thinking [56]	Reasoning	Qwen/Qwen3-Next-80B-A3B-Thinking
OpenAI	gpt-oss-120b [46]	Instruction	openai/gpt-oss-120b
	GPT-4o (\$) [1]	Instruction	-
	o1 (\$) [47]	Reasoning	-

Table 2: List of LLMs benchmarked as response generators in zero-shot prompting, RAG with abstracts, RAG with full-text, and VILLA.

Model Name	Context Length	Embedding Dimension	HuggingFace Model Name
Llama-3.1-8B	128K	-	meta-llama/Llama-3.1-8B
MedCPT (0.1B) [31]	64	768	ncbi/MedCPT-Query-Encoder
	512	768	ncbi/MedCPT-Article-Encoder
Qwen3-embedding:8B [56]	32K	4,096	Qwen/Qwen3-Embedding-8B
PubMedBERT (0.1B) [22]			NeuML/pubmedbert-base-embeddings
Open AI text-embedding-3-large	-	3,072	-
Google embeddinggemma-300M	2,048	768	google/embeddinggemma-300m
SFR-Embedding-Mistral (7B)	4,096	4,096	Salesforce/SFR-Embedding-Mistral

Table 3: List of LLMs benchmarked as embedders in RAG with abstracts, RAG with full-text, and VILLA.

Next, we embedded each semantic chunk using SFR-Mistral-7B [42] to obtain 4096-dimensional vector representations and indexed them in a FAISS vector store [32] for efficient semantic search based on vector similarity.

D Qualitative Evaluation

In the viral mutation extraction task, we prompted each model to retrieve the impact of each of the viral mutation on virus-host interaction apart from the mutations themselves. The different models reported this information in field named ‘reasoning’ which we manually evaluated to determine its quality and accuracy. We defined five rubrics and developed a user interface for this qualitative evaluation process.

D.1 Rubrics for evaluating LLM responses

To qualitatively assess the LLM reasoning responses, we developed a rubric with five categories: clarity, conciseness, correctness, citations/context, and contribution. All categories were measured on a five point scale, with one being the lowest score and five the highest. The first category, clarity, addressed how clearly ideas and arguments are expressed in the reasoning, focusing on the organization and coherence of the response. The second category, conciseness, addressed whether the reasoning text was efficient and purposeful to convey all relevant information. While total length was a consideration, we did not want to penalize reasoning that included more mutations. The third category, correctness, addressed whether the writing was mechanically correct and accurately identified mutations in the developed ground truth dataset. The fourth category,

citations/context, addressed whether the reasoning included citations and context that were relevant, authentic, and complete. The fifth category, contribution, was a holistic measure of the usefulness of the reasoning and addressed whether the mutations and context provided in the reasoning were significant to the understanding of host-virus interactions and correctly answering the query.

D.2 User interface for qualitative evaluation

We developed a web application to serve as the user interface for domain experts (virologists) to access, read, and evaluate the various model responses. Appendix Figure 8 and Appendix Figure 9 denote the interfaces to select a response of any model and evaluate the reasoning contents respectively. The administrator’s interface track the evaluations of all domain experts is shown in Appendix Figure 10.

D.3 Implementation

We used the open source persistent vector database called ChromaDb made available by LangChain³ to construct the vector datastores in RAG with abstracts, RAG with full text, and multi-level RAG experiments. We used DSPy framework⁴ to implement the Zero-shot evaluation, RAG with abstracts, RAG with full-text, and multi-level RAG methods. Unless stated, all figures denote the distribution of metrics across five iterations of viral mutation extraction for each of the ten influenza A proteins.

³<https://github.com/langchain-ai/langchain/tree/master/libs/partners/chroma>

⁴<https://github.com/stanfordnlp/dspy/tree/main>

ID	VIRUS	PROTEIN	STATUS	SUBMITTED
zmghjhrw60j	Influenza A	PB2	COMPLETED	Feb 3, 2026, 06:32 PM
c7jgmrwg7ms	Influenza A	PB2	COMPLETED	Feb 3, 2026, 06:13 PM
7h4gDuf1mkkg	Influenza A	PB2	COMPLETED	Feb 3, 2026, 06:10 PM
m1trj3k7m3ks	Influenza A	PB2	COMPLETED	Feb 3, 2026, 06:08 PM
zmghjblcy8b6c	Influenza A	PB1-F2	COMPLETED	Feb 3, 2026, 06:02 PM
c7jgmrwg7ms	Influenza A	PB1-F2	COMPLETED	Feb 3, 2026, 06:00 PM
7h4gDuf1mkkg	Influenza A	PB1-F2	COMPLETED	Feb 3, 2026, 05:58 PM
m1trj3k7m3ks	Influenza A	PB1-F2	COMPLETED	Feb 3, 2026, 05:56 PM
zmghjkm5j24	Influenza A	PB1	COMPLETED	Feb 3, 2026, 05:54 PM

Figure 8: The overview page on evaluation interface allows evaluators to filter, sort, and select outputs for review while tracking evaluation progress and mitigate selection bias. Features include searchable virus/protein filters, status indicators (pending/completed), flexible sorting options, and anonymized output identifiers that prevent cherry-picking and ensure comprehensive evaluation coverage.

GROUP	LLM OUTPUT ID	VIRUS NAME	PROTEIN NAME	MODE NAME	PRECISION	RECALL	CLARITY	CONCISENESS	CORRECTNESS	CONTEXTUALIZATION	CONTRIBUTION	ADDITIONAL COMMENTS
Group 1	zmghjkm5j24	Influenza A	PB1	response	0	4	4	4	1	5	-	
Group 2	zmghjblcy8b6c	Influenza A	PB2	response	0	4	1	3	3	4		
Group 3	c7jgmrwg7ms	Influenza A	PB2	response	0	4	5	5	4	5		
Group 4	7h4gDuf1mkkg	Influenza A	PB2	response	0	4	5	1	1	1		
Group 5	zmghjhrw60j	Influenza A	PB2	response	0	5	5	5	4	5		
Group 6	zmghjblcy8b6c	Influenza A	PB1-F2	response	0	4	1	2	3	2		
Group 7	c7jgmrwg7ms	Influenza A	PB1-F2	response	0	5	5	2	3	3		

Figure 10: The admin dashboard enables research oversight with tabular views of LLM outputs and evaluations, filtering by criteria ratings and metadata, CSV export functionality for data analysis, and enabling monitoring for tracking evaluation progress and ensuring data quality throughout the study.

LLM OUTPUT EVALUATION

Removing evaluator: 46 of 40 remaining | Output ID: zmghjblcy8b6c | [BACK TO LIST](#)

QUERY CONTEXT

Wink: Influenza A | Protein: PB1-F2

LLM OUTPUT

IDENTIFIED <ZOOTIC MUTATIONS>

CLARITY: 1 2 3 4 5

CONCISENESS: 1 2 3 4 5

CORRECTNESS: 1 2 3 4 5

ADDITIONAL COMMENTS (OPTIONAL):

Figure 9: The evaluation interface for each LLM output consists of two primary components: a fixed left panel presenting extracted mutations and associated reasoning, and a right panel containing a structured Likert-scale rubric with dynamic descriptive text and an optional comment box for additional feedback.

You are a virologist studying the evolution of viruses. The goal is to identify mutations in a virus that affect host shift in animals. Your job is to first read all scientific publications available in the literature about virus-host interaction in Influenza A. Next, you must identify all the mutations in the PB1 protein of the Influenza A virus that have an effect on the virus-host interaction. Finally, state the effect of the identified mutations on the virus-host interaction. Respond with all the mutations that have been reported to have an effect on the interaction between the Influenza A virus and any host along with the reasoning.

Your output fields are:

- mutations** (list[str]): list of all mutations in a viral protein. Mutations are listed as symbols in the format of <original amino acid><position><changed amino acid> where <position> denotes the position where the mutation occurs in the viral protein sequence, <original amino acid> is the alphabet representing the amino acid at that position in the viral protein sequence, and <changed amino acid> is the alphabet representing the changed amino acid. For example, "A123C" is a mutation of amino acid "A" to "C" at position "123".
Note: the value you produce must adhere to the JSON schema: {"type": "array", "items": {"type": "string"}}
- reasoning** (str): Effect of each identified mutation on the interaction between the influenza A virus and the host .

Figure 11: Prompt used to query large language models (LLMs) for viral mutation extraction using zero-shot prompting. The text highlighted in green denotes the key points such as description of the SIE task to respond with mutations impacting virus-host interaction in a given viral protein, the required output format, and the representation format of mutations.

E Viral Mutation Extraction Using Baseline Models

We compared the performance of nine different LLMs as response generators (responders) for SIE using zero-shot prompting, two implementations of RAG, and VILLA. Additionally, we evaluated seven LLMs as embedders for the RAG-based methods designed in this study.

E.1 Zero-shot prompting

Appendix Figure 11 shows the prompt used to query responder LLMs in a zero-shot manner for viral mutation extraction. Appendix Figure 12 shows the distribution of the number of mutations identified by each LLM, as compared to ground truth mutations for each of the ten influenza A proteins. The precision, recall, and

F1-scores of LLMs under zero-shot evaluation varied substantially across all the proteins (Appendix Figure 13).

E.2 Vanilla retrieval-augmented generation (RAG)

We implemented two types of RAG with the datastore containing (i) embeddings of abstracts and (ii) embeddings of chunks of full text from all 239 influenza A publications in ground truth dataset. Appendix Figure 14 shows the prompt in the RAG frameworks for viral mutation extraction. It includes instructions to extract the desired information from the provided context only.

Appendix Figure 15 denote the distribution of the precision and recall scores (averaged across ten influenza A proteins) of extracting the correct viral mutations using the two RAG implementations. It also contains the precision and recall scores of the retrievers for their ability to identify and include contents from the publications relevant to the given viral protein.

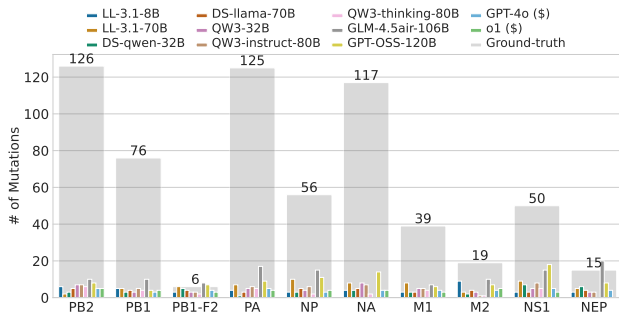


Figure 12: Distribution of the number of mutations identified by each of the eleven LLMs in ten proteins of the influenza A virus (x-axis) using zero-shot prompting. The gray bars denote the number of mutations in the ground truth known to impact virus-host interactions. The x-axis denotes the ten different influenza A proteins for which each LLM identified mutations. The height of each bar and the error mark in black correspond to the mean and standard deviation of the distribution respectively.

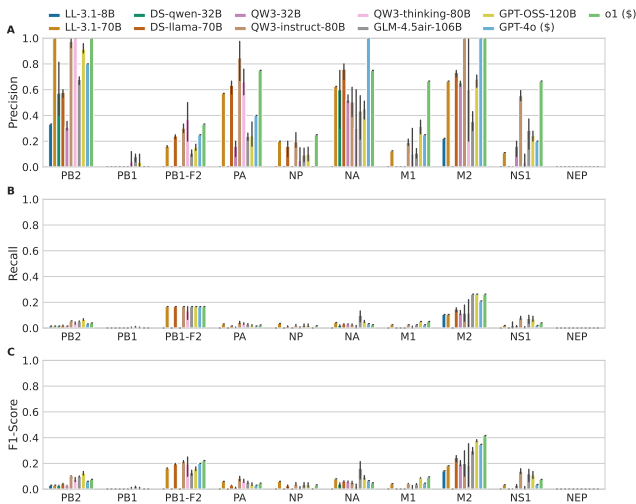


Figure 13: Distribution of the (A) precision, (B) recall, and (C) F1-scores of eleven general purpose LLMs in identifying mutations in influenza A virus that impact virus-host interaction. The x-axis denotes the ten different influenza A proteins for which each LLM identified mutations. The height of each bar and the error mark in black correspond to the mean and standard deviation of the distribution respectively.

E.2.1 RAG with abstracts. This section illustrates the performance of the RAG framework using only the abstracts of the scientific publications in the dataset, including the number of abstracts retrieved per protein and the precision, recall and F1-scores of publications retrieved in the context (Appendix Figure 16). We analyzed the number of mutations identified by different proteins for every protein and the corresponding precision, recall, and F1-scores for viral

You are a virologist studying the evolution of viruses. The goal is to identify mutations in a virus that affect host shift in animals. Your job is to first read the scientific literature provided in the context. Next, you must identify all the mutations in the PB1 protein of the Influenza A virus that have an effect on the virus-host interaction. Finally, state the effect of the identified mutations on the virus-host interaction. Respond with all the mutations that have been reported to have an effect on the interaction between the Influenza A virus and any host along with the reasoning.

Your input fields are:

1. "context" (str): contextual information for the question.
2. "question" (str): prompt to extract mutations for a given virus and protein combination from the given scientific literature in context.

Your output fields are:

1. "mutations" (list(str)): list of all mutations in a viral protein. Mutations are listed as symbols in the format of <original amino acid><position><changed amino acid> where <position> denotes the position where the mutation occurs in the viral protein sequence, <original amino acid> is the alphabet representing the amino acid at that position in the viral protein sequence, and <changed amino acid> is the alphabet representing the changed amino acid. For example, "A123C" is a mutation of amino acid "A" to "C" at position "123". Note: the value you produce must adhere to the JSON schema: {"type": "array", "items": {"type": "string"}}
2. "reasoning" (str): Effect of each identified mutation on the interaction between the influenza A virus and the host.

Figure 14: Prompt used to query large language models (LLMs) for viral mutation extraction using zero-shot prompting. The text highlighted in green denotes the key points such as description of the SIE task to respond with mutations impacting virus-host interaction in a given viral protein, the required output format, and the representation format of mutations. The text highlighted in blue instructs the LLMs to look only within the provided context while searching for answers.

mutation extraction (Appendix Figure 17). We also evaluated the performance of mutation retrieval at per protein level with respect to the ground truth mutations in the publications represented in the context (Appendix Figure 18).

E.2.2 RAG with full text. This section illustrates the performance of the RAG framework using the full text of the scientific publications in the dataset, including the number of publications represented in the context through the retrieved chunks for each protein and the corresponding precision, recall and F1-scores (Appendix Figure 19). We analyzed the number of mutations identified by different proteins for every protein and the corresponding precision, recall, and F1-scores for viral mutation extraction (Appendix Figure 20). We also evaluated the performance of mutation retrieval at per protein level with respect to the ground truth mutations in the publications represented in the context (Appendix Figure 21).

E.3 Viral mutation extraction using VILLA

This section illustrates the performance of the multi-level RAG framework involving both abstracts and the full text of the scientific publications in the dataset. We analyzed the number of mutations identified by different proteins for every protein and the corresponding precision, recall, and F1-scores for viral mutation extraction (Appendix Figure 22). We also evaluated the performance of mutation retrieval at per protein level with respect to the ground truth mutations in the publications represented through the abstracts identified in the level one of retrieval (Appendix Figure 23).

We used Qwen3-Embedding:8B as the embedder LLM to compare the distribution of cosine distances between the embeddings of abstracts and the embedding of a prompt for viral mutation extraction in each influenza A protein (Appendix Figure 24). Appendix Figure 25 shows the performance of different combinations of six LLMs as embedders and nine LLMs as response generators in identifying mutations in influenza A virus that impact virus-host

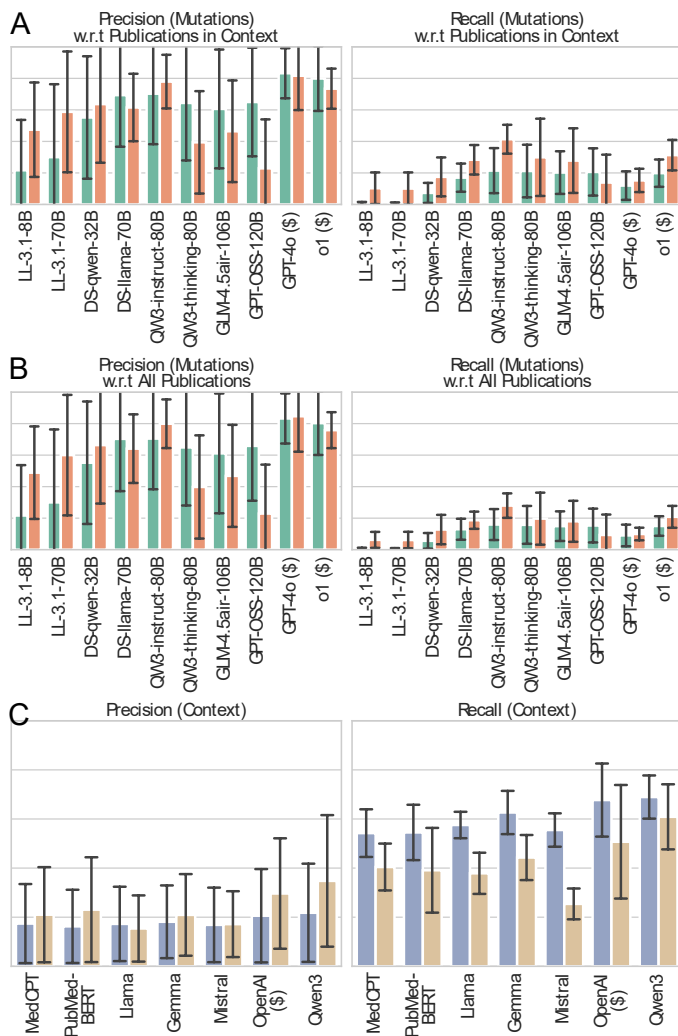


Figure 15: Distribution of the (A) precision and recall with respect to the ground truth mutations in the publications represented in the context in the prompt and (B) the ground truth mutations in all the publications. The scores are for ten LLMs evaluated using RAG with abstracts and RAG with full text in identifying mutations across ten proteins in influenza A virus. (C) Distribution of the precision and recall scores of the retriever in the two RAG frameworks in identifying abstracts relevant to each of the ten proteins in influenza A virus. The retriever is evaluated using seven different embedding LLMs. Each bar height and error bar corresponds to the mean and standard deviation of the distribution respectively. Abbreviations: LL, Llama; DS, DeepSeek; QW3, Qwen.

interaction using multi-level RAG method. Additionally, we performed hyperparameter analysis to determine the optimal values for number abstracts (k_a), and number of chunks (k_c) in the two levels of retrieval in VILLA respectively (Appendix Figure 26).

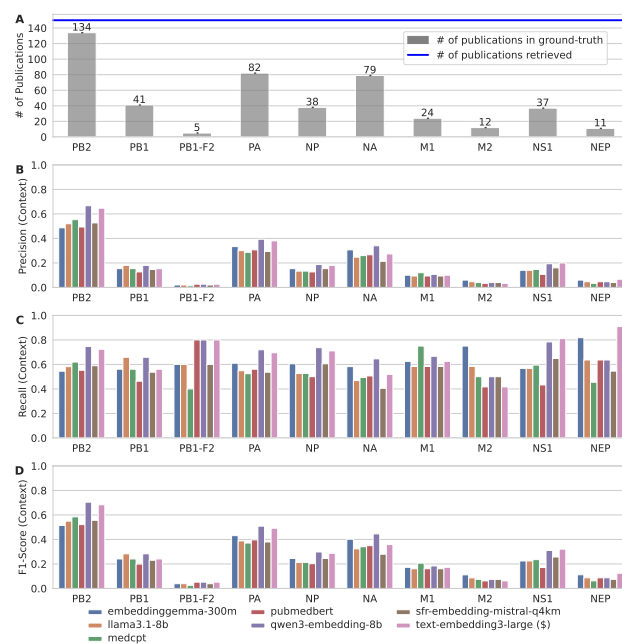


Figure 16: (A) The gray bars denote the number of abstracts in the ground truth relevant to each of the ten proteins (x-axis). The solid blue line indicates the number of abstracts retrieved for each protein. Distribution of the (B) precision, (C) recall, and (D) F1-scores of the publications represented in the context of each prompt when querying to retrieve mutations in influenza A viral proteins using RAG with abstracts method. The performance of seven different embedding LLMs are compared through the evaluation of the context. The x-axis denotes the ten different influenza A proteins for which each LLM identified mutations. The height of each bar and the error mark in black correspond to the mean and standard deviation of the distribution respectively.

F Benchmarking SIE Methods for Viral Mutation Extraction

VILLA performed significantly better than zero-shot prompting, RAG with abstracts, and RAG with full-text when we used nine different LLMs as the response generators. Our proposed method also outperformed state-of-the-art RAG- and agent-based tools namely, OpenScholar [2], PaperQA2 [54], and HiPerRAG [20] (Appendix Figure 28).

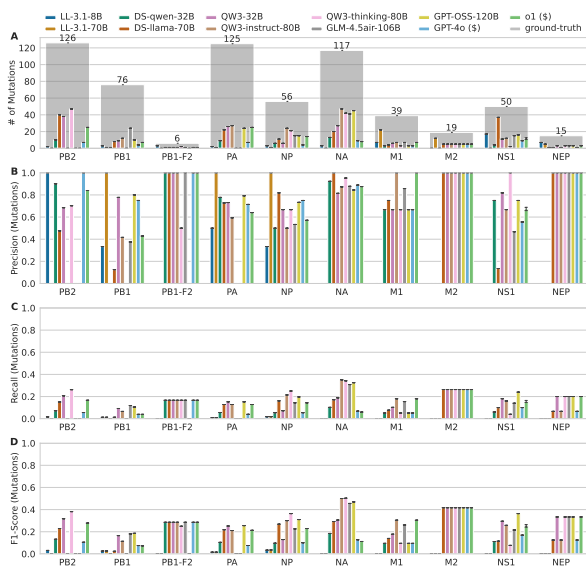


Figure 17: (A) Distribution of the number of mutations identified by each of the eleven LLMs in ten proteins of the influenza A virus (*x*-axis) using RAG with abstracts. The gray bars denote the number of mutations in the ground truth known to impact virus-host interactions. Distribution of the (B) precision, (C) recall, and (D) F1-scores of eleven general purpose LLMs in identifying mutations in influenza A virus that impact virus-host interaction using RAG with abstracts method. The metrics are computed with respect to all the corresponding ground truth mutations of a given protein. The *x*-axis denotes the ten different influenza A proteins for which each LLM identified mutations. The height of each bar and the error mark in black correspond to the mean and standard deviation of the distribution respectively.

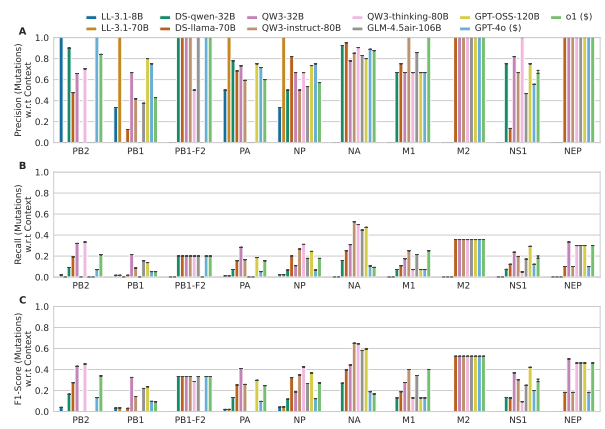


Figure 18: Distribution of the (A) precision, (B) recall, and (C) F1-scores of eleven general purpose LLMs in identifying mutations in influenza A virus that impact virus-host interaction using RAG with abstracts method. The metrics are computed with respect to the ground truth mutations in the publications represented in the context of each prompt. The distribution is across five iterations of SIE for each of the ten proteins. The *x*-axis denotes the ten different influenza A proteins for which each LLM identified mutations. The height of each bar and the error mark in black correspond to the mean and standard deviation of the distribution respectively.

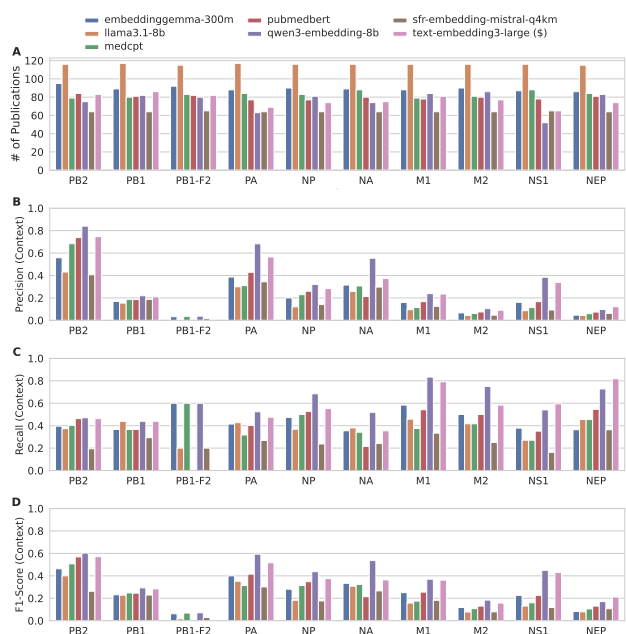


Figure 19: (A) Number of publications retrieved in the context for each of the ten influenza A proteins. The number in parentheses below every protein name in the x-axis denotes the number of publications in the ground truth dataset relevant to each of the ten proteins. The colored bars show the number of publications identified by the retriever using the embeddings from seven different embedder LLMs. Distribution of (A) precision, (B) recall, and (C) F1-scores of the publications represented in the context of each prompt when querying to retrieve mutations in influenza A viral proteins using RAG with full text method. The performance of seven different embedding LLMs are compared through the evaluation of the context. The x-axis denotes the ten different influenza A proteins for which each LLM identified mutations. The height of each bar and the error mark in black correspond to the mean and standard deviation of the distribution respectively.

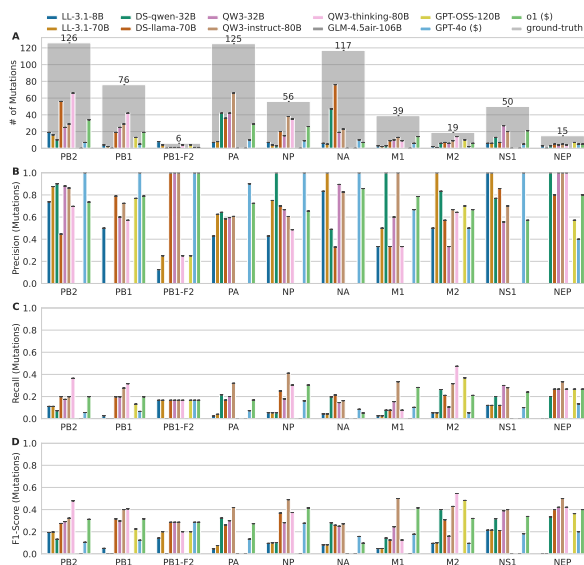


Figure 20: (A) Distribution of the number of mutations identified by each of the eleven LLMs in ten proteins of the influenza A virus (x-axis) using RAG with full text of the publications. The gray bars denote the number of mutations in the ground truth known to impact virus-host interactions. Distribution of the (B) precision, (C) recall, and (D) F1-scores of eleven general purpose LLMs in identifying mutations in influenza A virus that impact virus-host interaction using RAG with full text method. The metrics are computed with respect to all the corresponding ground truth mutations of a given protein. The x-axis denotes the ten different influenza A proteins for which each LLM identified mutations. The height of each bar and the error mark in black correspond to the mean and standard deviation of the distribution respectively.

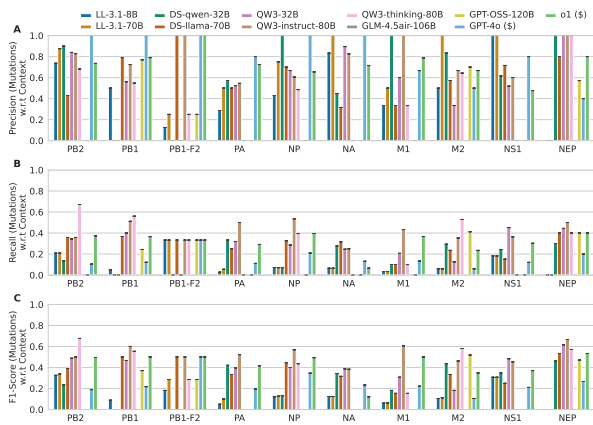


Figure 21: Distribution of the (A) precision, (B) recall, and (C) F1-scores of eleven general purpose LLMs in identifying mutations in influenza A virus that impact virus-host interaction using RAG with full text method. The metrics are computed with respect to the ground truth mutations in the publications represented in the context of each prompt. The x-axis denotes the ten different influenza A proteins for which each LLM identified mutations. The height of each bar and the error mark in black correspond to the mean and standard deviation of the distribution respectively.

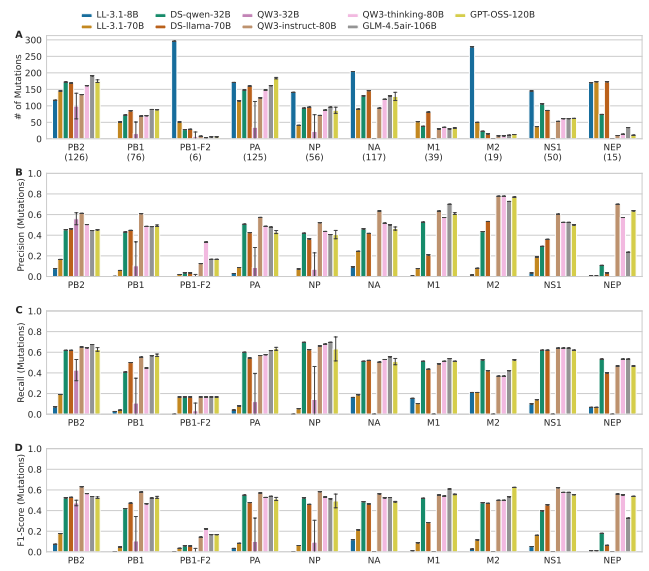


Figure 22: (A) Distribution of the number of mutations identified by each of the eleven LLMs in ten proteins of the influenza A virus (x-axis) using RAG with full text of the publications. The number in parentheses below every protein name in the x-axis denotes the number of mutations in the ground truth known to impact virus-host interactions. Distribution of the (B) precision, (C) recall, and (D) F1-scores of eleven general purpose LLMs in identifying mutations in influenza A virus that impact virus-host interaction using multi-level RAG method. The metrics are computed with respect to all the corresponding ground truth mutations of a given protein. The x-axis denotes the ten different influenza A proteins for which each LLM identified mutations. The height of each bar and the error mark in black correspond to the mean and standard deviation of the distribution respectively.

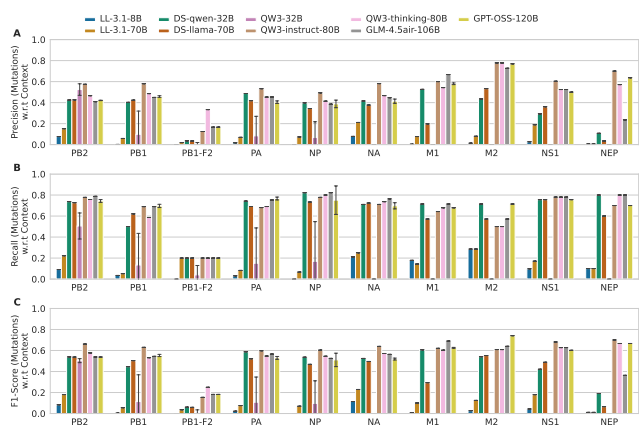


Figure 23: Distribution of the (A) precision, (B) recall, and (C) F1-scores of eleven general purpose LLMs in identifying mutations in influenza A virus that impact virus-host interaction using multi-level RAG method. The metrics are computed with respect to the ground truth mutations in the publications selected in the first retrieval step. The x-axis denotes the ten different influenza A proteins for which each LLM identified mutations. The height of each bar and the error mark in black correspond to the mean and standard deviation of the distribution respectively.

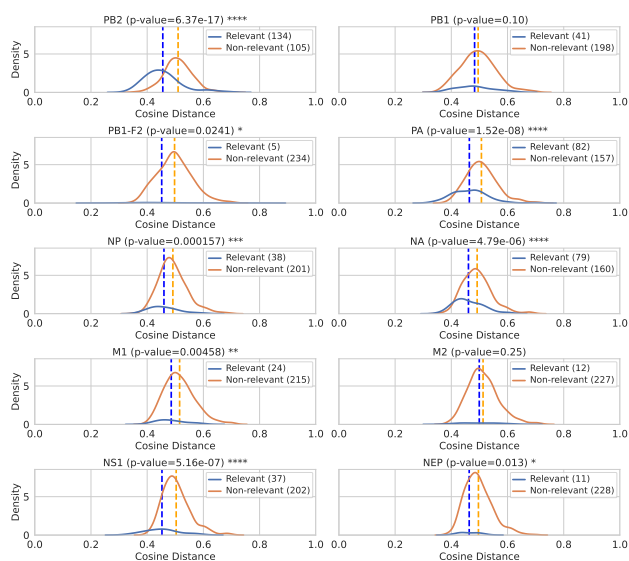


Figure 24: Comparison of the distribution of cosine distances between the embeddings of abstracts and the embedding of a prompt for viral mutation extraction in given influenza A protein. Each subplot corresponds to one of the ten proteins. The dashed vertical lines in blue and orange denote the mean cosine distance of the relevant and non-relevant abstracts from the prompt respectively. All embeddings were computed using Qwen3-Embedding:8B LLM. For each protein, the p -value denotes the statistical significance of the two distributions begin different.

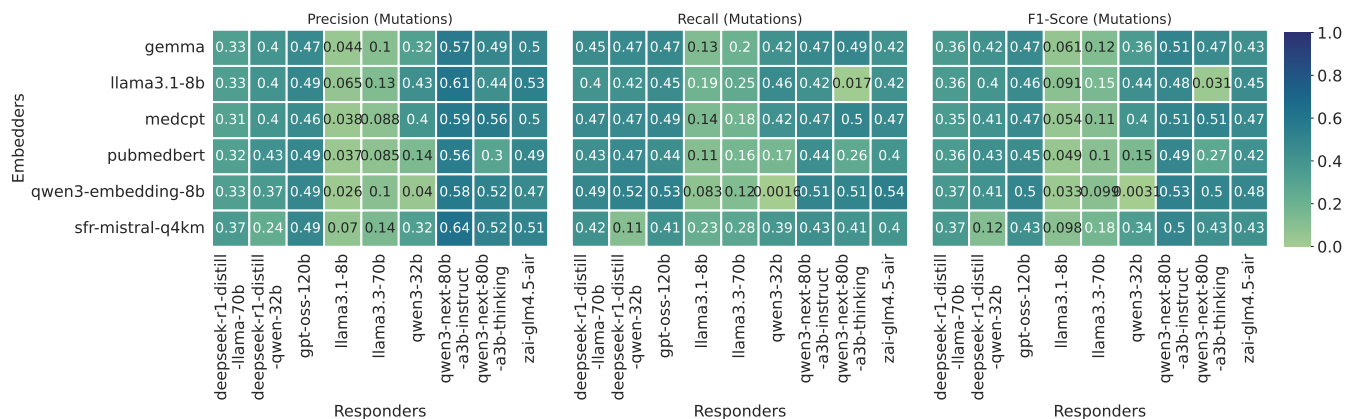


Figure 25: Performance of different combinations of LLMs as embedders and response generators in identifying mutations in influenza A virus that impact virus-host interaction using multi-level RAG method. In each heatmap, the rows correspond to six different embedder models, and the columns denote nine different response generators. Each cell shows the average precision, recall, or F1 score across five iterations of SIE for each of the ten influenza A proteins.

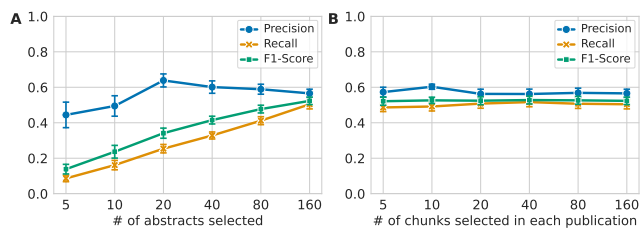


Figure 26: (A) Precision, recall, and F1-Scores for different values of number of abstracts selected in multi-level RAG with the number of chunks selected in each publication fixed at 160. (B) Precision, recall, and F1-Scores for different values of number of chunks selected from each publication in multi-level RAG with the number of abstracts selected fixed at 160. In both sets of experiments, the embedder and responder models were ‘Qwen3-Embedding-8B’ and ‘Qwen3-Next-80B-A3B-Instruct’ respectively. The scores are for identifying mutations across ten proteins in Influenza A virus. The x-axis denotes the different values of the hyperparameter. Each point in the line and the error bar denote the mean and standard deviation of the corresponding distribution respectively.

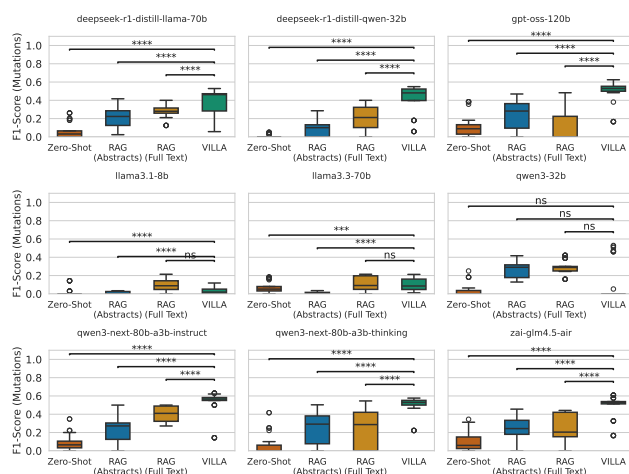


Figure 27: Comparison of F1-scores in SIE of mutations in influenza A virus using zero-shot prompting, RAG with abstracts, RAG with full text, and multi-level RAG methods. Each sub-plot corresponds to a comparison of the methods using a different LLM for response generation. Each box-plot is a distribution of the F1-scores from five iterations of retrieving mutations in ten influenza A proteins using ten different prompts. The stars and ‘ns’ denote the statistical significance computed using Mann-Whitney U test as follows, $p\text{-value} \leq 1e-4$: ‘****’; $1e-4 < p\text{-value} \leq 1e-3$: ‘***’; $1e-3 < p\text{-value} \leq 1e-2$: ‘**’; $1e-2 < p\text{-value} \leq 5e-2$: ‘*’; $p\text{-value} > 5e-2$: ‘ns’ (not significant).

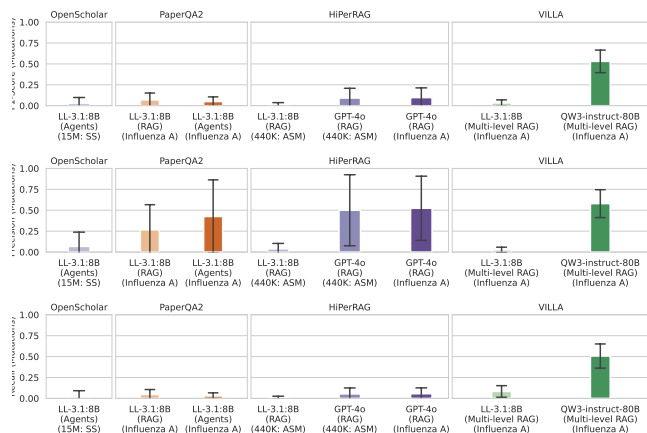


Figure 28: Distribution of the precision, recall, and F1-scores of OpenScholar, PaperQA2, HiPerRAG, and VILLA frameworks in retrieving mutations of influenza A viral proteins. The y-axis denotes the different configurations of frameworks analysed. Each subplot corresponds to one type of SIE method with different configurations represented using different shades. Bars with lighter shade correspond to flavors of methods with Llama 3.1:8B as the response generator (responder). Bars with darker shades denote the performance of the best configuration for the respective method namely, full agentic framework for paperQA2, GPT-4o as responder for HiPerRAG, and Qwen3-Next-80B-A3B-Instruct as responder for VILLA. Each bar height and error bar corresponds to the mean and standard deviation of the distribution respectively.